Iraqi Journal of Civil Engineering

Journal homepage: https://ijce.uoanbar.edu.iq/

A Review of the Flexural Behavior of Steel-Concrete Composite Beam Specimens Fabricated with Different Concrete Strengths Experimentally and Numerically

Husam Khalaf Khudhair Al-Ani [a], Ameer Abdulrahman Hilal[a], Sheelan Mahmoud Hama[a]*

[a]*Department of Civil Engineering, College of Engineering, University of Anbar, Anbar, Iraq*

PAPER INFO

ABSTRACT

Composite beams, made up of a concrete slab and steel in the IPE steel section, are commonly used in bridges and buildings. Their main function is to enhance structural efficiency by merging the compressive strength of concrete with the tensile resistance of steel, thereby improving overall stiffness, ductility, and load-bearing capacity. This study offers an extensive review of the flexural behavior of steel-concrete composite beams, focusing on the interplay of concrete strength, shear connector types, and interaction levels in determining structural performance. It integrates experimental and numerical research to analyze critical parameters, including load-deflection behavior, shear transfer efficiency, and crack propagation at the steel-concrete interface. The study emphasizes the effect of concrete compressive strength, particularly in ultra-high-performance concrete (UHPC) and lightweight concrete, on stiffness, ductility, and load-bearing capacity while reducing self-weight and enhancing sustainability. The study revealed that fully bonded shear connectors, using CFRP sheets and welded plates, enhance flexural capacity and stiffness. In contrast, partial bonding or pre-debonding reduces performance due to crack propagation. Indented and hot-rolled U-section connectors enhance interaction and minimize slip, while uniform distribution of shear connectors optimizes load capacity and stiffness. Lightweight concrete decreases slab weight without compromising performance, and high-performance materials such as ECC, SFRC, and UHPFRC improve strength and ductility. Numerical modeling, particularly finite element methods, and higher-order beam theories validate experimental results, providing accurate tools for predicting structural behavior under various loading and environmental conditions.

* Corresponding author. Tel.: +0-000-000-0000 ; fax: +0-000-000-0000.
E-mail address: hus21e1001@uoanbar.edu.iq

1. Introduction

Steel-concrete composite girders are frequently utilized in constructing bridges and buildings to flexure as the primary structural members. Typical composite steel-concrete structures include columns, beams, and slabs that combine the best structural characteristics of both materials. For instance, composite steel-concrete beams consist of a beam of steel exposed mainly to tensile stresses and a concrete part placed above the flange and exposed to compressive stresses. The fact that each material is used to take advantage of its positive attributes makes composite steel-concrete construction very efficient and economical (Muteb & Rasoul, 2016). In buildings, multiple-story, steel, and concrete elements are commonly utilized. Concrete slabs over steel beams are an example of this. The same applies to road bridges, where concrete decks are normally preferred. To what extent the parts or components of a construction consist of all steel components, are made wholly from reinforced concrete, or are made from composite materials will be based on the circumstances. Undoubtedly, engineers tend to more and more design composite building systems by combining reinforced concrete and steel sections to create more structurally sound if comparing designs made from only one material (Wald, Zadonini, & Jaspart, 2000). Generally, steel-concrete composite systems are considered the most cost-efficient systems in construction for multiple-story buildings. Structural effectiveness comes from effectively employing structural materials, particularly concrete and steel, thus eliminating their main drawbacks. Meanwhile, enhancing the speed of construction because the need for props and formwork can be greatly minimized or possibly entirely avoided. Nevertheless, even with all the benefits and advantages of structural systems based on composite material, they have yet to be implemented widely, which is certainly not as widely as it should be (Dujmovic, Androic, & Lukacevic, 2015). Composite steel-concrete beams are often preferable for designers due to their high percentages of strength to weight. Although the system of composite steel-concrete beams presents benefits regarding flexural capacity relative to ordinary reinforced concrete beams, because of the reduction in self-weight achieved by the steel beam, the system can be applied to longer spans (Ferreira, Tsavdaridis, Martins, & De Nardin, 2021; Shao, Deng, & Cao, 2019), for example, bridge structures with long spans and parking structures (Jakovljević, Spremić, & Marković, 2023). Similarly, composite steel-concrete beams can be employed to accelerate the process of construction (Wang, Zhang, Zhou, Zhang, Chen, & Li, 2022; Ma, Lou, & Bao, 2022; Yang & Xie, 2023). For accelerating the construction of bridges, steel-concrete composite I-girders are often used. The pre-fabrication of composite steel-concrete I-beam girders is widely used for their functional benefits, economy, and accelerated structural construction (Lin, Liu, & Roeder, 2016; Mosallam, Feo, Elsadek, Pul, & Penna, 2014; Su, Yang, & Bradford, 2015). Pre-fabrication for composite steel-concrete beams also allows exploiting the latest bridge materials and technologies developed in line with the most recent research and development (Yoo & Choo, 2016; Henderson, Zhu, Uy, & Mirza, 2015). In the composite girder, stud shear connectors are utilized to bond the slab/deck of reinforced concrete to the steel flange of the I-girder. Consequently, it significantly reduces deflection and greater moment resistance and has a smaller steel section relative to simple steel systems having a greater span-over-depth percentage (Vasdravellis, Uy, Tan, & Kirkland, 2012; Ataei, Bradford, & Liu, 2016).

The nature and characteristics of concrete and steel differ, although both are complementary and compatible. From a mechanical perspective, properly combining them would allow us to take advantage of their respective capabilities and associations. In terms of thermal expansion, they have almost the same properties and a perfect strength combination since concrete has a high compression strength, and steel has a high tensile strength. Concrete likewise provides anti-corrosion protection and insulating properties for the steel in high temperatures and may also prevent thinner steel sections from buckling in local or lateral directions. Using composite structures allows for the integration of concrete and steel under the condition that a composite action is present between the steel sections and concrete. The behaviour of the steel-to-concrete connection plays a vital role in the overall structural element behaviour. A composite action could be achieved by minimizing or eliminating the relative displacements between steel elements and concrete in their interface. To make the two elements (a steel beam and a concrete slab) work as a single element, it is necessary to use shear connectors to avoid slippage at the interface between steel and concrete. Typically, shear connectors with headed studs are the most commonly utilized because of their simplicity in welding and installation (Du, Hu, Meng, Han, & Guo, 2020; Oehlers & Bradford, 1995).

The design of composite beams ensures that the maximum strength of either the concrete slab or steel beam under axial force and bending occurs earlier than the shear interface fails (Oehlers, Nguyen, Ahmed, & Bradford, 1997; Park, Kim, Lee, & Choi, 2013; Bärtschi, 2005). Even so, a slip along the shear interface can cause the beam to fail early. As a result of the flexibility of the connectors, partial interaction happens, and the shear connectors number necessary for full interaction cannot be accommodated (Park, Kim, Lee, & Choi, 2013). Early in loading,

partial interaction permits the composite beam to perform in the same manner as if it had been fully connected. However, the shear connection fails to transfer the shear force under greater loads, eventually producing a slip along the shear interface. Thus, partial interaction could greatly decrease the composite beam's flexural resistance because of slip along the shear interface. Shear connectors are mainly responsible for steel-to-concrete connections' behavior. Various shapes and configurations of shear connectors influence the force transfer between the steel and concrete sections and contribute to their deformation. As a result, the main differences between different kinds of connectors are strength capacity, stiffness, and deformation ability (Oehlers, Nguyen, Ahmed, & Bradford, 1997; Zeng, Jiang, & Zhou, 2019; Daou, Mahayri, Daou, Baalbaki, & Khatib, 2021; European Committee for Standardization, 2004).

This study aims to provide a comprehensive review of the flexural behaviour of steel-concrete composite beams, focusing on the influence of concrete strength, shear connector types, and interaction levels on structural performance. By consolidating experimental and numerical findings, the study highlights critical parameters such as load-deflection behaviour, shear transfer efficiency, and crack propagation at the steel-concrete interface. It also aims to assess the role of advanced materials like ultra-high-performance concrete (UHPC) and lightweight concrete in enhancing composite action while identifying gaps in the current understanding of sustainability, long-term behaviour, and dynamic performance. The goal is to propose directions for future research and provide insights to improve the design, efficiency, and durability of composite beam systems for modern engineering applications.

2. Historical Background

During the mid-20th century, early studies highlighted the fundamental composite action between steel and concrete, emphasizing improvements in load-bearing capacity and ductility. As a result of advances in materials and structural analysis techniques, extensive research was conducted in the 1970s and 1980s on shear connection mechanisms, stress distribution, and experimental validation. This research is ongoing, with further studies contributing to understanding time-dependent effects such as creep and shrinkage, allowing for a comprehensive long-term performance analysis. In recent years, finite element modeling has provided deeper insight into structural behavior, enabling the refinement of design methods. In structural applications, these developments have profoundly impacted modern design codes and practices, ensuring the reliability and effectiveness of steel-concrete composite beams.

3. Flexural Behaviour of Steel-Normal Concrete Composite Beams

Sallam's team studied the influence of separation before the intermediate level on the flexural performance of composite steel-concrete beams strengthened with either a sheet of carbon fiber reinforced polymer (CFRP) bonded with adhesive or a steel plate bonded by welding. Eight identical composite steel-concrete beam specimens were fabricated. In the scenario of strengthening using a CFRP sheet, two distinct modes of attachment, a CFRP sheet encircled and enveloping the I-beam flange and a CFRP sheet encircling and enveloping the flange along with a section of the web, have been investigated through testing four types of strengthened composite steel-concrete beam specimens undergoing bending at four points. Two beam specimens are strengthened with two forms of a completely attached CFRP sheet. In contrast, the rest were the same but had a debonding zone before the intermediate by a length of 50 mm on the lower flange's bottom surface. In the scenario of strengthening by a steel plate, three kinds of attachment configurations of steel plate on beam soffits, which include non-continuous welded, welded at the end, and bonded along with welded steel plates, have also been tested undergoing bending at four points. To perform the shear connection between the steel beams and concrete part, shear studs in two rows of longitudinal patterns in 12 mm and 50 mm diameters were utilized and welded on steel beams at the top flange, as shown in Fig. 1. The concrete has been designed to achieve a 40 MPa compressive strength following 28 days. Two rows of steel bars with a diameter of 12 mm have been employed to reinforce the concrete slab. There were four longitudinal bars and 20 transverse bars in every layer.

The experimental outcomes revealed that, following yielding, the beams containing the pre-debonding region exhibited lesser flexural strength than those containing complete bonding because the intermediate debonding developed quickly. Meanwhile, yield loads differed between the welded steel plate configurations, with a modest change in elastic stiffness. The behavior of the relation for load-to-strain turns inaccurate when the steel yields at

the location of the strain gauge. Beams that have been strengthened using steel plates or CFRP sheets were unaffected by the separation at the intermediate. In all CFRP-sheet strengthened beams, the debonding at the intermediate begins its development beyond the steel flange's yielding (Sallam, Badawy, Saba, & Mikhail, 2010).
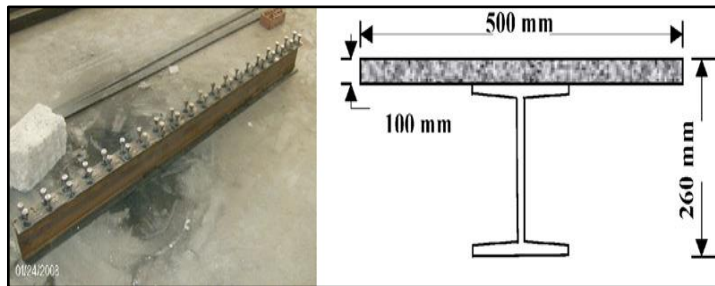

Fig. 1 I-beam after welding two rows of shear stud and cross-section dimensions

Alves's group present a future investigation of the performance of composite beams made of steel and concrete. A continuous shear connector with linear indentation, commonly known as Crestbond, was utilized to connect the concrete part to the steel beam to guarantee these components' joint integrity. The study involves a numerical and experimental approach where the numerical analysis was performed using the ATENA three-dimensional analysis program. The experimental experiments and the numerical modeling have been conducted to assess the composite beam performance and, especially, the shear connector with the indented shape in the composite beam behavior analysis. The experimental specimens comprise a steel beam equipped with a connector in a continuous indented pattern placed above the upper flange, continuously welded throughout, and a slab made of reinforced concrete. Tested composite beams had been simply supported and spanned 3000 mm long, as shown in Fig. 2. The beams consisted of an IPE200 steel section, a composite slab of 400×100 mm2 cross-section, and a shear connector featuring a continuous indentation. Loading was carried out using a four-point configuration. Two identical loads were imposed symmetrically, with the space in between being 60 cm, equivalent to one-fifth of the length of the span. Regarding the geometry of the connector, the CR40-R10 Crestbond, as revealed in Fig. 3. was designed according to the dimensional specifications suggested by Veríssimo (2007), measuring 70 mm in height, enough to support slabs up to 100 mm thick. There was an 84 mm distance between the centers of the connector slots. The connector has been positioned in a symmetrical state across the span of the beam and in line with the steel profile web. The compressive strength and modulus of elasticity were 38.1 MPa and 31.56 GPa at 29 days.

Results demonstrated that the beam ends experienced nearly no damage, and observing uplift deformation or slip at the cross-section above the supports was not feasible. For the two tested composite beam specimens, the failure happened in the upper slab portion as crushing in concrete and a large vertical displacement arising in the middle of the beam span. Both beams exhibited the same behavior, achieving an ultimate load of 284.7 kN and 284.3 kN. Both extremities of the same beam had similar slip values and were the same for both tested composite beams. The ultimate value of slip amounts to (0.15 and 0.13 mm) indicates that these values are relatively small and that the connector of the indented shape has a high degree of stiffness. Additionally, the low values of slip suggest that the connector of the indented shape has a high level of interaction with the cross sections of concrete and steel. Experimental and numerical findings have been very closely matched. As for behavior during the elastic stage, there seems to be close to a complete agreement between both numerical models and experimental data. The strain values developed in the beams tested experimentally and the models of numerical analysis resemble each other, apart from the ultimate load stage, where the experimental values were greater than the numerical ones. The numerical findings demonstrate that the yielding of a steel beam occurs roughly at the same time as longitudinal cracks in the composite slab begin. The tests confirmed the excellent efficiency of the connector of the indented shape utilized in the composite beam specimens, and the created model of numerical analysis was a valuable guide for additional parametric investigations (Alves, Isabel, Washintgon, & Gustavo, 2018).
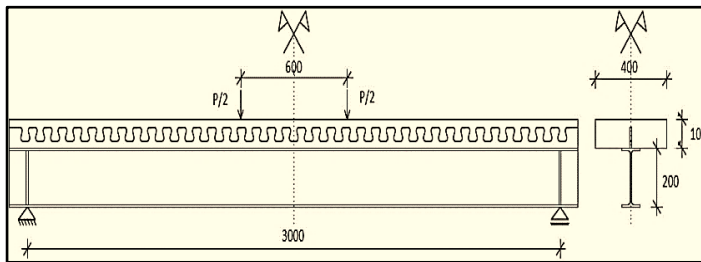
Fig. 2 Geometry of the composite beam (in mm)   **Fig.3 Dimensions for the Crestbond**
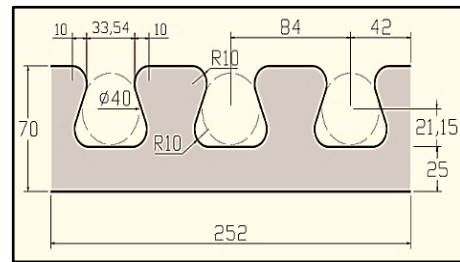
Ribeiro Neto, Vieira, and Zoccoli (2020) compared the structural performance of composite steel-concrete beam specimens for three kinds of shear connectors fabricated in a hot-rolled U section and U and L sections fabricated by cold-formed. To investigate the performance of the connectors that act direct on the concrete slab-steel beam interface, similar composite beam specimens have been constructed for every kind of connector, with electrical strain gauges being the only difference between each pair. Tests conducted in experimental work have been fabricated using the three types of shear connectors, as demonstrated in Fig. 4., connected with laminated steel beams of I-section and slabs fabricated from reinforced concrete. The shear connectors have been evenly distributed, excluding those close to the beam end, maintaining the greatest distance prescribed by the European Committee for Standardization (2004), as illustrated in Fig. 5. Six tests for beams in a simple supported state were conducted to assess the positive bending at the moment zone. The compressive strength values are 32.7, 33.9, and 35 MPa.

The outcomes demonstrate considerable differences in the performance of direct shear among the various kinds of connectors. Despite this, they do not considerably affect the mean flexural capacity of the composite beam specimens. The U 3"x6.1 connector provides a 46% greater carrying capacity relative to the U 76x36x4.75 connector; in turn, it was 24% larger in strength compared to the L 76x36x4.75 connector. The carrying capacity of the U-shaped hot-rolled and L-shaped cold-formed sections differs by about 76%. The stiffness difference among the sections has been directly correlated with its strength capacity. A great rigidity for the section correlates with more section strength and will make the steel section and slab less likely to slide relative to each other. For the entire specimens nearly, the cracks formed in the middle of the slabs, spreading across two-struts of compression when compared to the greatest slab dimension. Some modes of failure have been unidentified, leading to speculation that the rupture of the concrete could have happened beyond the connector sliding excessively. The stiffness of composite beams is significantly influenced by relative sliding. In the beam specimen with greater interaction, displacement from the theoretical analysis tended to be a little larger relative to displacement in the experimental test. If the degree of interaction of the beam specimens was near 0.3, the displacements measured experimentally were near the theoretical values on average. Thus, it can be inferred that U and L sections fabricated in cold form are suitable for utilization in composite beams as shear connectors; however, in the construction procedure, it is necessary to consider their low strength capacities and stiffness relative to laminated U sections. Their use is discouraged in the case of high-loading composite beams or high stiffness requirements, such as in dynamic structural systems.

Fig. 4 Beam and connectors   **Fig. 5 Positioning of shear connectors on the beam**
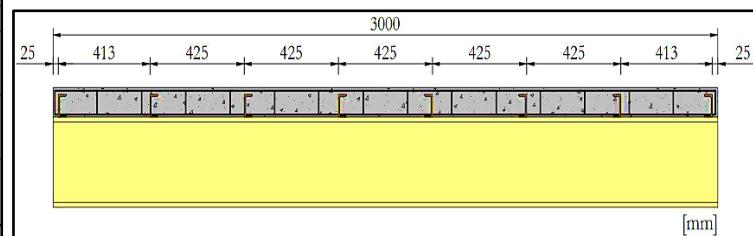
Zhou, Uy, Li, and Liu (2021) conducted an extensive experimental, analytical, and numerical investigation on the behavior of composite beams made of stainless steel and concrete. The bending experiments comprised eighteen concrete-stainless steel composite beam specimens with a full size that were manufactured and designed per AS/NZS 2327 (Australian/New Zealand Standard, 2017). Fig. 6 exhibits a composite beam cross-section. The specimens comprised a concrete panel, a beam of welded stainless steel, and many shear connectors. The concrete panel has been designed with a width of 600 mm and a thickness of 100 mm. The mid-span was prone to pure bending conditions in the bending test from four points and could provide a distribution of stress and strain under a pure moment. However, the test for bending in three points involves a complex stress scenario, and the effect on the behavior of the bending due to shear stress has been noticed. The specific details of loading and setting up the instrument for three-point and four-point loading were illustrated in Figs 6, b, and c. As part of the test of shear, a total of six shorter composite beams have been fabricated in different lengths (A and B) based on the four-point bending tested specimens (as seen in Fig. 6, c) to obtain multiple degrees of shear connection for the subsequent shear tests of three-point bending. Four Specimens were tested under combined bending and shear in a combined bending-shear test. The effective length Le of composite beam specimens has been adjusted to produce different degrees of shear and moment. In these tests, each specimen has been designed to serve as composite beams subjected to testing under loading in three points. A 3-D finite element FE model has been created in ABAQUS, and numerical simulations have been conducted to support the experimental work. The moment capacity of composite beam specimens made of stainless steel and concrete has been calculated by new models analytically. The average strength of the compressive concrete on the 28th of its testing days measured 42 MPa.

All specimens were subjected to tests of bending, shear, and a combination of bending and shear, demonstrating a high degree of ductility due to the properties of members of stainless steel. The composite beam specimens from stainless steel and concrete incorporating bolted shear connectors demonstrated the same maximum moment resistance as welded stud specimens. Despite this, the first had a lower flexural stiffness because of the clearance between the bolt and the hole. The maximum shear strength of composite beam specimens from stainless steel and concrete incorporating welded studs and bolted shear connectors tended to be similar. Still, shear strength may be diminished by a lower degree of shear connection. Compared with the existing codes of practice AS/NZS 2327 (Australian/New Zealand Standard, 2017) and EN1994-1-1 (Johnson & Anderson, 2004) designed for carbon steel composite beams, the stainless steel-concrete composite beam could sustain higher flexural capacity owing to its remarkable strain hardening effects. The design strategy described in AS/NZS 2327 was exaggerated in calculating the shear strength of composite beam specimens of the stainless steel due to the premature failure of concrete, limiting the strength of stainless steel from developing. A method for designing stainless steel has been suggested based on utilizing a lowered strength of stainless steel, which yielded conservative estimates of the shear strength. The design strategies outlined in EN 1994-1-1 and AS/NZS 2327 may offer a reasonable assessment of the behavior of composite beam specimens of stainless steel and concrete for the interaction of moment and shear.
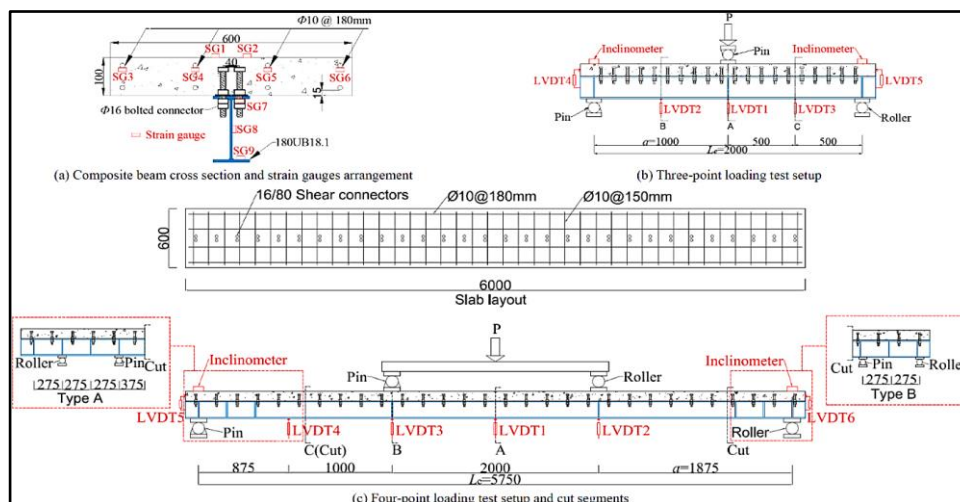

Fig. 6 Setting up configuration and equipment for a tested composite beam.

4. Flexural Behaviour of Steel-High Strength Concrete Composite Beams

Muteb and Rasoul (2016) investigated the structural performance of composite beams of ultra-high-performance concrete steel when loaded with monotonic load. The investigation has been performed with a theoretical and experimental approach. Seven composite beams were tested for a point load in the experimental part. These beams were divided into two categories depending on variable attributes. The first category contained four beam specimens; one beam was the reference one, designed to represent partial contact, and the remaining beam specimens contained several numbers of shear connectors. The second category contained three beam specimens depending on the varying shear connector distribution in the shear zone only. The specimens being tested have been modeled numerically and analyzed through the finite element approach in the numerical section. All beams were simply supported and tested under two-point loads, as shown in Fig.7. No reinforcement was used in the concrete slab, and the distribution of shear connectors in one row in the longitudinal direction.

Overall, the results revealed that the ultimate load increased with increasing the shear connectors, and the measured end slip value decreased when the degree of partial shear connection rose from 41.6% to 58.3% to 83.3% up to 100%. It concluded that the decrease in the spacing of shear connectors to a minimum has no effect. The measured end slip value decreased when the degree of partial shear connection increased to 100%. The increase in the number of connectors in the ends increased the slip stiffness of the beam. The predicted failure loads from the numerical analysis were nearly identical to those obtained during the experimental test. The findings of the finite element model analysis exhibited a good match with those of the experimental work.
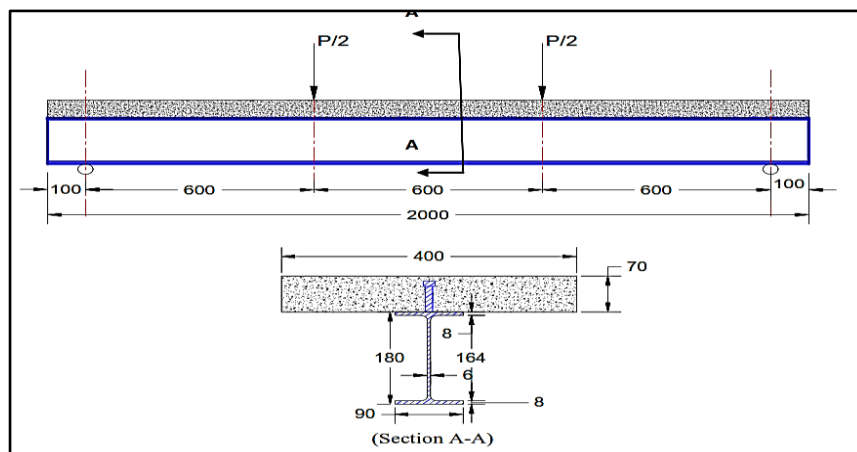
Fig. 7 Dimensions of Composite Beam Specimens (all dimensions in mms).

Hamoda, Hossain, Sennah, Shoukry, and Mahmoud (2017) investigated the performance of composite girders fabricated with steel beams of the I section connected by the shear connectors of a stud shape to the slab of high-performance concrete. Various concrete types were utilized for making four specimens of composite girders, and those with varying slab continuities were tested up to failure using static loading to simulate negative moments, as exhibited in Fig.8, a. To obviate early steel I-beam lateral buckling that possibly stopped the test, based on the recommendation of Vasdravellis's work (Vasdravellis, Uy, Tan, & Kirkland, 2012), eight stiffeners were set in web and welded on both sides of the I-shaped steel beam, and constructed fly bracing was fastened with bolts of high-tensile steel, as clarified in Fig. 8, b. The composite action was completed using thirty-two-headed shear studs (80 mm high and 10 mm diameter) to connect the robust steel I-beam of the W150 37 section. Headed shear studs were welded in two lines along the upper flange as well as including three studs positioned at both ends to minimize the early slip, as demonstrated in Fig. 9. Two bolts with high-tensile steel and in-place castings were also utilized for the slab connection process. Concretes of three kinds were used for the first three specimens of a steel girder, including Normal Concrete (NC), Steel Fiber-Reinforced Concrete (SFRC), and engineered cementitious composite (ECC). The fourth specimen of the steel girder was fabricated using two end slabs of SFRC joined with a closure strip of Ultra-High-Performance Fiber-Reinforced Concrete (UHPFRC) at the mid-length region where the highest negative moment was present.

The girder beam with SFRC and ECC exhibited 23% and 12% greater elastic stiffness, in that order, relative to their counterparts with NC. In contrast, the girder specimen fabricated with SFRC- a UHPFRC closure strip demonstrated increased stiffness by 19%. The specimen girder constructed with the ECC exhibited a stiffness of 11% less than its counterpart with SFRC. The cracking loads for girder specimens SFRC and ECC were 51% and 16% greater than their counterpart with NC, respectively, whereas the SFRC girder cracking load was 30% higher than the ECC one. Furthermore, the composite girders specimens fabricated with SFRC and ECC demonstrated 72% and 21% greater yield loads, in that order, than those with NC. The greater load of reinforcement-yielding is likely due to the effect of fiber bridging on the cracks in the concrete matrix, which postponed the transfer of load to the reinforcement. The girder specimen using a UHPFRC strip demonstrated approximately 42% greater yield load compared to the counterparts with NC free off a closure strip. A girder specimen with ECC exhibited a 30% greater final deflection and a 42% smaller yield load than the girder specimen with SFRC. Girders specimens made of ECC had around 94% and 400% greater strain in concrete at the cracking phase than those with SFRC and NC, respectively, evidence that demonstrated excellent strain hardening and ductility properties of ECC. Each specimen failed because of the compression flange local buckling of the steel beam beyond the concrete slab cracking completely, the steel reinforcement yielding and the steel I-beam yielding at the location of maximum moment.

(a)   (b)
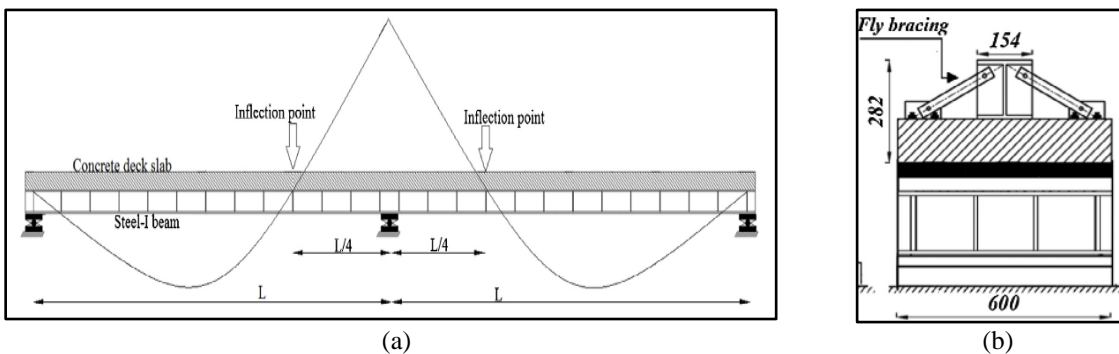
Fig.8 Setup of the test and total girders dimensions: (a) Negative moment area (in between turning points), (b) cross-section of specimens.

Fig. 9 Arrangement shear studs.

Liu, Lai, and Xu (2020) investigated experimentally the flexural behavior of composite girder specimens with laminated concrete and a steel girder. The deck made from laminated concrete comprises a layer of reinforced concrete (RC) and a layer of ultra-high-performance concrete (UHPC), and the composite girder made from laminated concrete-steel section has been labeled as the S-RC-UHPC girder. First, experiments were performed to evaluate the flexural performance of three specimens from composite girders: a steel-reinforced concrete (S-RC) girder, a steel-ultra high-performance concrete (S-UHPC) girder, and an S-RC-UHPC girder, as clarified in Fig. 10. A steel-reinforced concrete-UHPC composite girder (S-RC-UHPC) comprised of steel girders, a precast

reinforced concrete layer, and a cast-in-place UHPC layer, as illustrated in Fig.11, a, which also shows the elevation view of the specimens. The percentage of height over diameter for each stud complied with the guidelines of AISC360–16 (American National Standard, 2016) (which means the percentage must be higher than or equal to 4). Two rows of shear studs connected the steel girder and the concrete deck. These shear studs have been arranged transversely at 85 mm and longitudinally at 110 mm, as exhibited in Fig. 11, b.

Specimen S-RC-UHPC exhibited great strength and equivalent stiffness compared to specimen S-RC despite being constructed of a 20% smaller concrete deck and demonstrated a great stiffness and strength relative to the S-RC specimen. Furthermore, the S-RC-UHPC specimen featured less material cost than the S-UHPC specimen and was lighter in weight than the S-RC specimen. Therefore, S-RC-UHPC girders will be more efficient for use from either S-RC or S-UHPC girder. A similar failure mode was identified in all three tested girders (S-RC-UHPC, S-RC, and S-UHPC), including the yielding of the steel girder, tension concrete cracking, and the concrete crushing in compression. Until the maximum load, the S-RC-UHPC specimen showed no slip or separation along the interface between the precast reinforced concrete and layers of UHPC. Consequently, the presence of complement in work between the two laminated layers can be concluded. The influence of shear lag in these composite girder specimens increased in response to increasing loads and decreased when UHPC was utilized. As a whole, the slip was relatively small in all tested girder specimens. The use of UHPC can effectively decrease slip, as demonstrated by S-RC-UHPC and S-UHPC specimens.
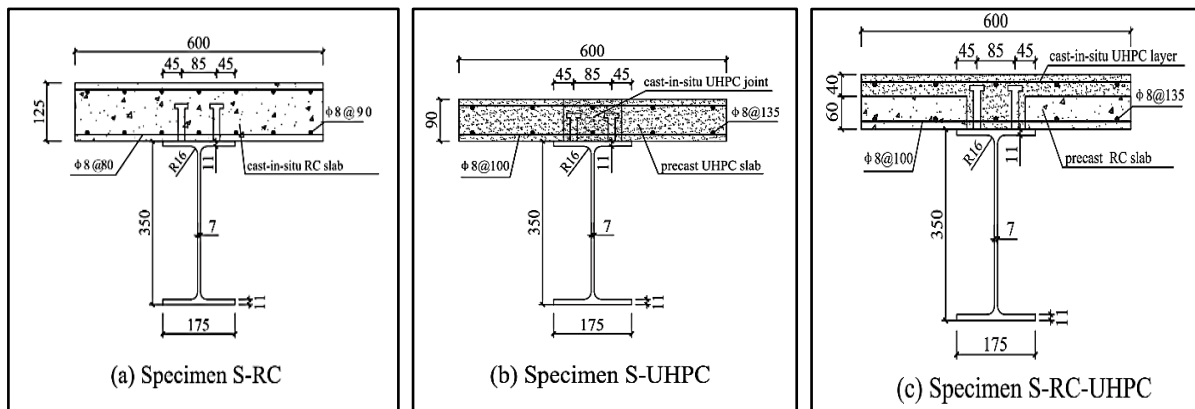
Fig. 10 Cross-section details of the specimens (unit: mm)
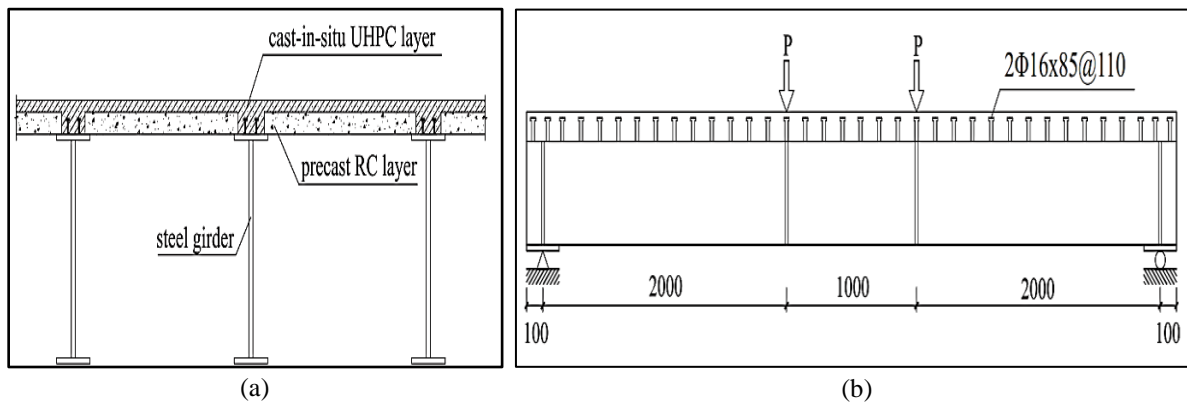
Fig. 11 Composite girders; (a) standard example of S-RC-UHPCm, (b) geometry of specimens (in mm).

Yoo's team aimed to evaluate the flexural behavior of composite beams comprising inverted-T steel girders and ultra-high-performance concrete (UHPC) slabs while considering the effects of partial interaction between the girders and the slabs. Eight full-scale specimens were tested under varying configurations to examine the

influence of stud spacing and slab thickness on the structural performance. These specimens were subjected to three-point bending tests, and parameters such as deflection, strain, and slip were measured using strain gauges and LVDTs. Web-mounted studs were employed to connect the UHPC slab and the inverted-T steel girder of the composite beam specimen, as demonstrated in Fig. 12. To complement the experimental findings, so, the current investigation suggested a nonlinear analysis approach for evaluating the flexural performance of the composite beam specimens in consideration of partial shear connection. The analysis approach used the Fourier series for internal forces approximation in a beam when the slip was considered was combined with the sectional analysis method, which accounted for the steel girder's inelastic behavior and the UHPC's nonlinear behavior.

The members of the composite beam specimen having a shorter stud distance interval performed monolithically because of the lower slip development. By contrast, the members having a larger stud distance interval demonstrated lower performance because of premature stud damage resulting from the higher degree of slip created from the partial interaction. Based on the relations between load and deflection, as well as load and concrete strain, the analysis suggested that the shear connection is ideal-rigid adequately to reproduce the behavior of the composite beam specimen with studs in a dense arrangement, contrary to this, the partial interaction analysis offered a better simulation in the composite beam specimen featuring a wide spacing between the studs. Regarding the composite beam specimen constructed from a UHPC slab and an inverted-T steel girder, the recommended spacing must be between 100 mm and lower than four times the slab thickness. Hence, it meets the ductile behavior limit of Eurocode-4 (Yoo, Choi, Choi, & Choo, 2021).
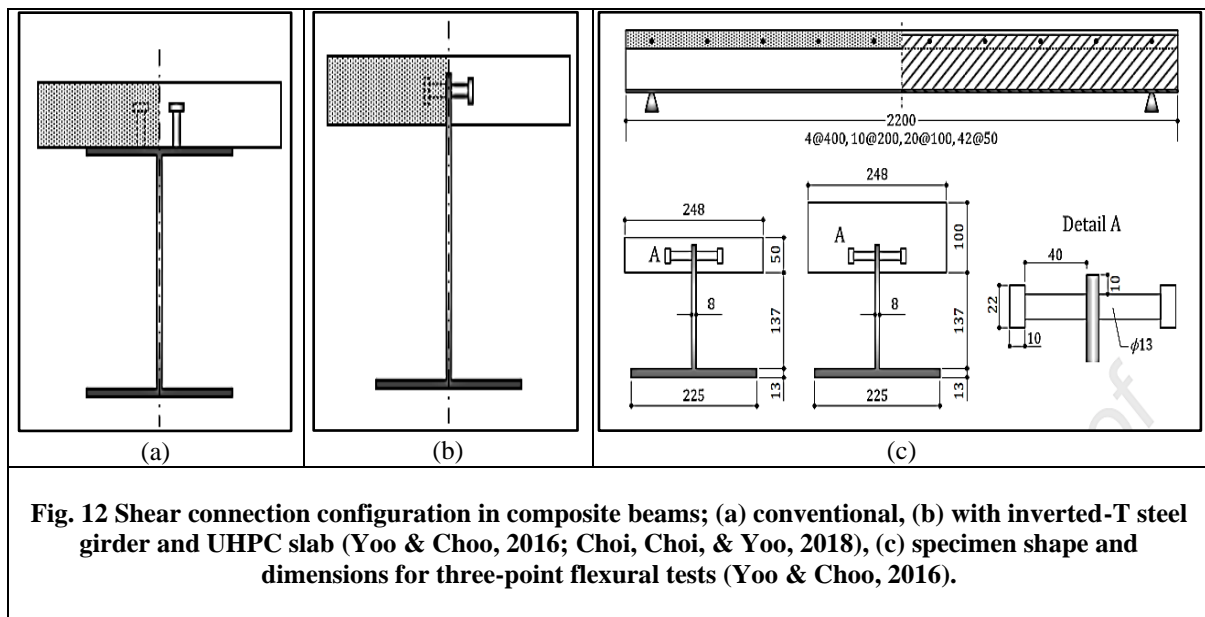
Fig. 12 Shear connection configuration in composite beams; (a) conventional, (b) with inverted-T steel girder and UHPC slab (Yoo & Choo, 2016; Choi, Choi, & Yoo, 2018), (c) specimen shape and dimensions for three-point flexural tests (Yoo & Choo, 2016).

Yang's group prefabricated four steel-concrete composite beams (PSCCBs) containing shear connectors as grouped bolts have been fabricated and tested to assess their flexural behavior when exposed to bending moments in the positive direction. The influence of the degree of shear connection and slabs with segmented precast concrete (PC) on the flexural behavior of PSCCBs has been evaluated. Shear connectors in bolt shape were installed in two rows along the girders and were utilized for transferring shear forces between steel girders and PC slabs. Bolts were arranged as groups of four, and the bolts in each group were spaced 80 mm transversely and 100 mm longitudinally. Fig. 13 clarifies how the PSCCBs have been assembled, and Fig. 14 illustrates the PSCCB's geometric dimensions and the slab reinforcement distribution. The modulus of elasticity and compressive strength for the used concrete in the slab was 39.6 GPa and 62.3 MPa, respectively.

Experimental findings demonstrated that the entire specimens failed because of steel girders yielding and crushing concrete in the middle of the span, reflecting flexural failure in typical form. The PSCCBs featuring segmented PC slabs exhibited a short, mid-span deflection increasing stage beyond the yielding of steel girders through the tests versus the PSCCB that featured a monolithic PC slab, in which the and coefficient of ductility and initial flexural stiffness dropped about 44.1 and 47.8% at highest, respectively. The maximum flexural strength went up as the degree of shear connection rose; on the other hand, the ductility of the beams declined.

Close to the gaps, there have been more relative slips observed. When segmented PC slabs were used instead of monolithic ones, the integrated flexural behavior of PSCCBs tended to deteriorate. When enlarging the width of the gap, the middle PC slab length and height of the girder web would be helpful for the PSCCB's ductility (Yang, Zhou, & Liu, 2023).
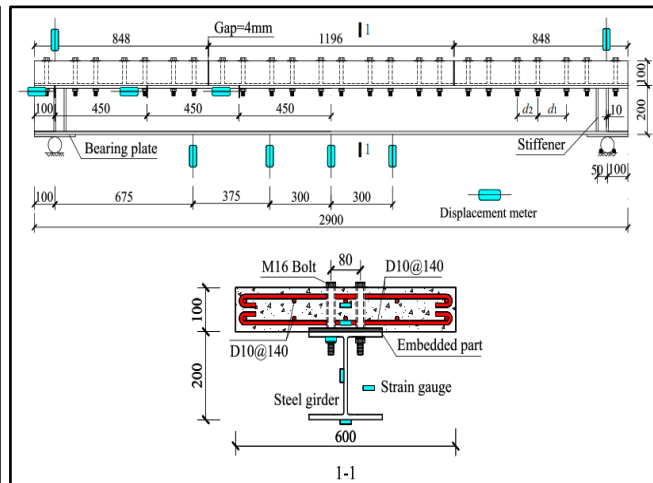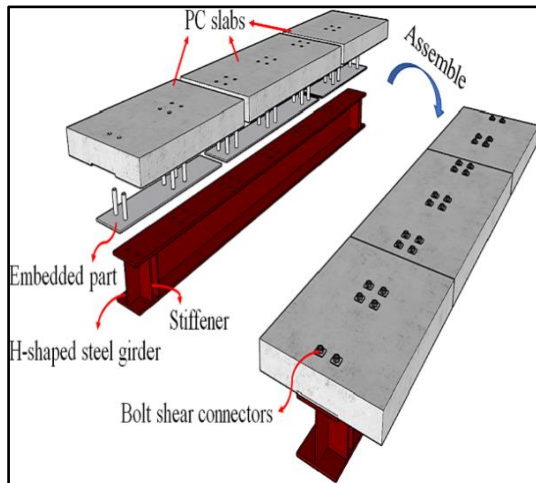

<table>
<tr><td>**Fig. 13 An assembly process diagram**</td><td>**Fig. 14 Details of dimensions and reinforcement (mm).**</td></tr>
</table>

5. Flexural Behaviour of Lightweight Steel-Concrete Composite Beams

Valente (2007) tested composite beam specimens made of lightweight concrete and steel under static and cyclic loading conditions. The cross-section of the tested beam consists of a typical steel profile and a concrete solid slab like section S4, diagrammed in Fig. 15, a. The opted slab had a cross-section of 350 mm by 60 mm. The size for the steel section was chosen according to the classification of composite cross-section under EN1994-1-1 (European Committee for Standardization, 2004) and the neutral axis location within the concrete slab based on plastic analysis. The tested beams had concrete characterized by lightweight and high strength. Around 60 MPa was the compressive strength of lightweight concrete LWC. Several disposition types for shear connections were tested to assess the influence of designing in the scenario of full and partial connections. Along the length of the beam, shear stud connectors have been evenly distributed. Shear connection is provided with equally spaced stud connectors of 13 mm diameter and 50 mm high. The shear connectors' distribution has three types, exhibited in Fig. 16, b. With Type A, steel connectors are uniformly distributed between the concrete slab and the steel profile. Type B connector distribution was intended to provide a partial connection between the steel profile and the concrete slab; therefore, failure should be expected along the connection line. In type C, connectors are arranged in pairs to connect the steel profile and concrete slab fully. The objective of the current work is to obtain better ductility for the shear connection of the beam (Döinghaus, 2001; Hegger, Sedlacek, Döinghaus, Trumpf, & Eligehausen, 2001). The load was applied in two configurations (Loading-1 and Loading-2) and the beam structural schemes for these loading cases have been illustrated in Figs: 16, a and b.

The performance of composite beam specimens with lightweight concrete and steel equipped with shear connectors of headed studs' style has been comparable with what to predict for concrete with normal density, even though not equal. Instead of crushing in concrete close to the stud location, the shear stud failed. Only beams containing double stud arrangement revealed cracks in the concrete slab adjacent to the stud locations. The equally spaced and evenly distributed studs were demonstrated to be the most effective connection type, providing a greater load capacity. Studs grouped in pairs permitted a greater vertical deformation; however, this reduced load capacity. In all cases, the beams designed to have full connection failed through concrete crushing at the cross-sections exposed to higher stresses. Partial-connection-designed beams experienced a higher level of slip deformation. In these situations, failure was associated with shear, which was always located on one specific beam

side. All the tested beams experienced ductile failure since they underwent high deformations while maintaining their load capacity.
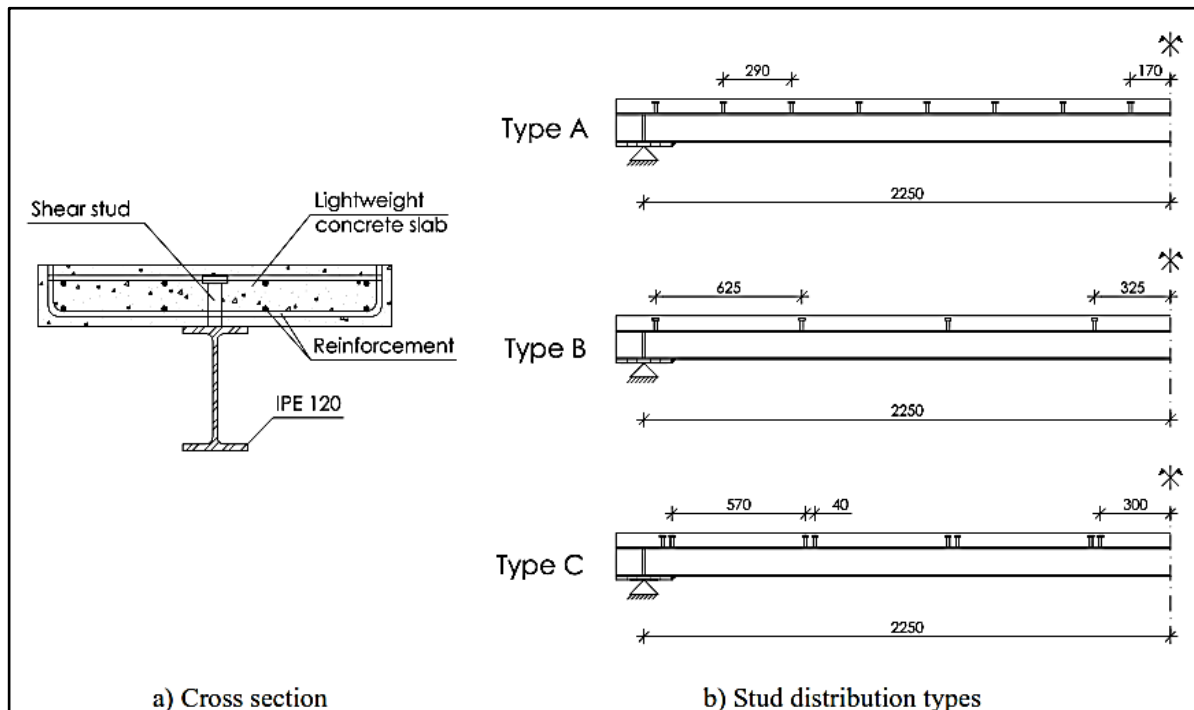

**Fig. 15 Types of cross-sections and stud disposition.**
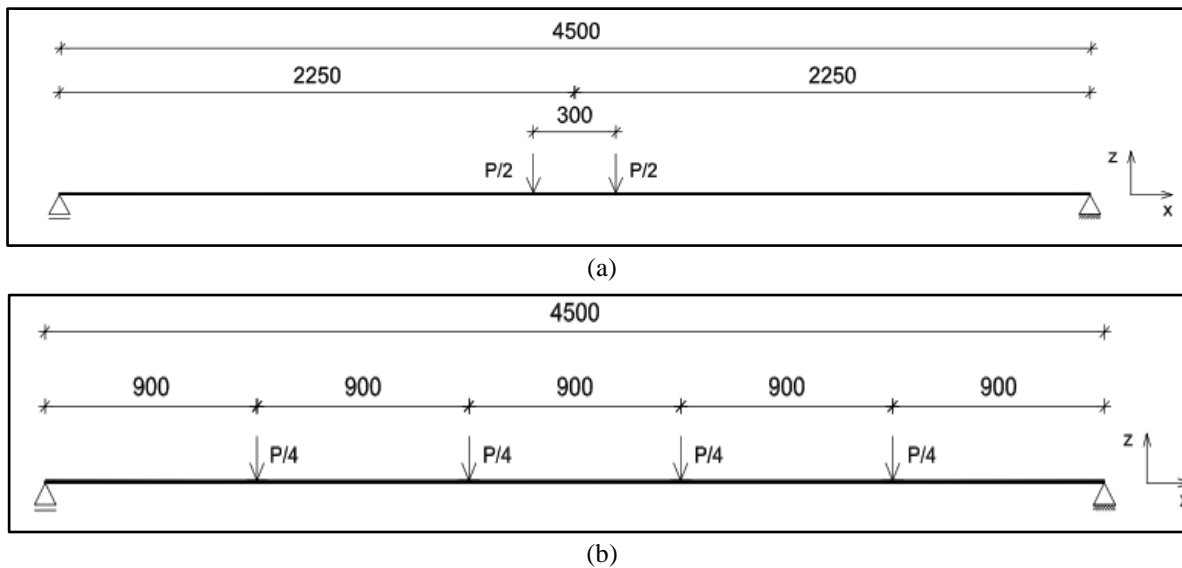
Fig. 16 Loading type; (a) Loading-1 structural scheme, (b) Loading-2 structural scheme.

Valente and Cruz (2010) discussed the experimental tests on steel and lightweight concrete composite beams. The primary intent has been to explain the behavior of composite beams, illuminate their shear connection, and investigate the role of the varying components in the deformation and load capacity. The investigation involved

testing composite beam specimens with a 4.5 m span with identical geometrical arrangement, materials, and simple state of support condition. The geometrical layout for the beam's cross-section and support was similar for whole beams. Fig. 17 reveals that the beam consists of an IPE120 steel section and a slab of lightweight concrete measuring 350×60 mm. The shear connection was made through evenly distributed studs with a diameter of 13 mm and a height of 50 mm. The shear connectors distribution is of three types: (1) total connection (8 studs ø13, h=50mm, in half span of the beam); (2) total connection associating connectors in pairs aiming a more ductile behavior of the connection (8 studs ø13, h=50mm, in half span of the beam) (Hegger, , Sedlacek, Döinghaus, Trumpf, & Eligehausen, 2001); and (3) partial connection (4 studs ø13, h=50mm, in half span of the beam). Two load configurations were considered, as exhibited in Fig. 18. The variables considered in the current work were the arrangement of studs and the type of load distribution.

On a global level, good behavior was observed, similar to that anticipated for concrete with a normal density. The connection between steel and concrete exhibited good behavior, as shear connection failure always occurs in place of concrete breaking adjacent to the stud location. The even and equally spaced arrangement of studs was the preferred efficient connection technique, providing a greater load strength. Studs grouped in pairs permitted higher vertical displacement yet led to a lower load strength. A limit state analysis can predict load and corresponding bending moment failure values. According to the European Committee for Standardization (2004), bending failure is considered for beams with total connection design, and the total plastic behavior of the transversal section at failure is accepted. In the beam design with a part-connection scenario, failure of the shear connection was recognized, contributing to a lower value for the ultimate bending moment. All the beams show an initial elastic behavior, approximate to estimate by an elastic approach, considering a total shear connection. For the Loading-1 group, the beam vertical displacement associated with the ultimate determined bending moment was similar for each type of total connection disposition despite the different loading levels. The ultimate bending moment for the Loading-2 group was identical for both full connection beam specimens; however, the peak vertical displacement was greater. The slip values measured for Loading Group-1 were generally higher than those for Loading Group-2 because the total load had been higher.
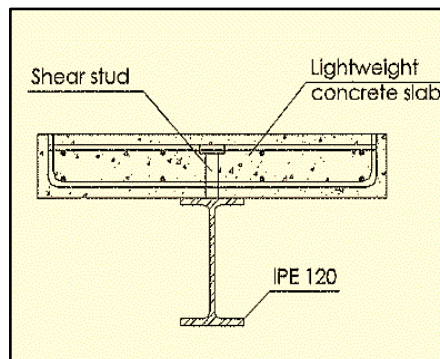

Fig. 17 Transeverse section
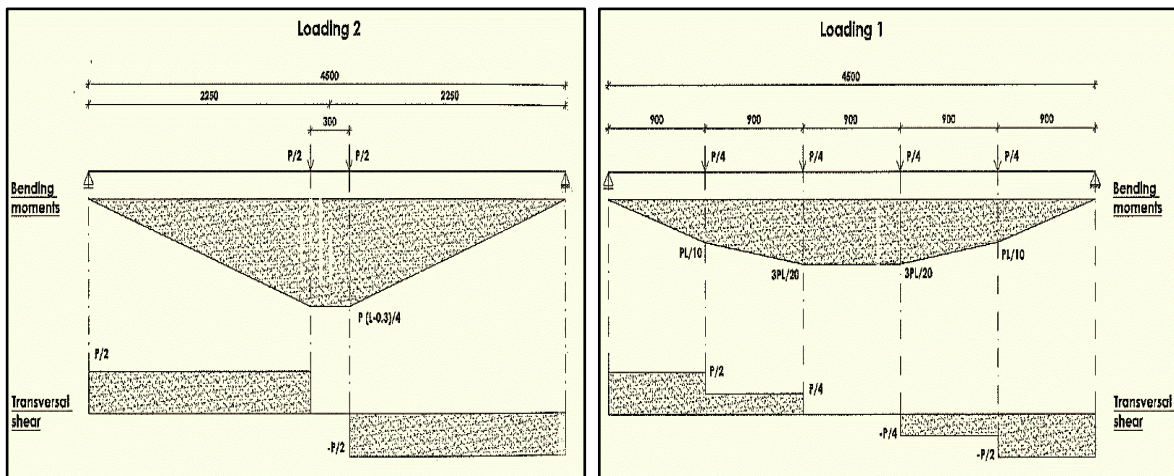
Fig. 18 Diagrams illustrating shear forces and bending moments corresponding to loads.

Lasheen, Shaat, and Khalil (2016) conducted an experimental study investigating the validity of lightweight concrete slabs in steel-concrete composite beams and comparing their behavior with normal-weight concrete slabs. Eight beams, comprising concrete slabs and steel sections utilizing channel connectors made of welded steel, were tested experimentally in the current study. The specimen's details are exhibited in Fig. 20, which consists of concrete slabs that are 80 mm in thickness. Longitudinally and transversely, concrete slabs were reinforced using a mesh of steel bars with a diameter of 8 mm and a spacing of 200 mm. The span length of six beam specimens was 4800 mm, whereas the span lengths of two were 2800 mm and 1800 mm. Seven beam specimens were manufactured utilizing an LWC density of 18.5 kN/m3. An NWC beam featuring a density of 23.5 kN/m3 has been fabricated for comparison purposes. The dimensions of the concrete slab were designed to guarantee that there would be no concrete crushing before failure happened to investigate the LWC slab's behavior during elastic and plastic stages. A linear distribution of stress along the depth of the beam has been supposed to design the composite beam specimen then adopted.

It was observed that lightweight concrete could effectively be used instead of normal-weight concrete. This reduced the concrete slab weight by 22%, with a marginal reduction in both the yielding and ultimate load capacities of the composite beams. The effects of the thickness of the concrete slab and modulus of elasticity were marginal on the slab's effective width because of the position of the concrete slab near the centroid of the composite section. The effective ratio of width-over-span for the concrete slab was significantly influenced by the steel beam slenderness ratio (L/rs). The width-over-span ratio decreased when the beam's slenderness ratio was raised. The concrete's effective width depended on the stage of loading. As a rule of thumb, the effective width considered in strength design (at maximum) was larger than in service loads by about 35%. In composite beam specimens, LWC possesses a minimal impact on ductility. Steel beams with small slenderness ratios utilize wider portions of concrete slabs. The widening of concrete slabs improved the ductility of beams, as an increase of 20% in the width of the slab led to a 32% improvement in ductility. Reduction of the account of needed shear connectors to 50% decreased the beam stiffness by just 5.5% because of the LWC's lower Young's modulus. The same lowering in shear connectors improved the ductility of the beam by approximately 25% without affecting the maximum load. Moreover, using LWC allows a considerable reduction in the required shear connectors without affecting the stiffness of the composite beams.
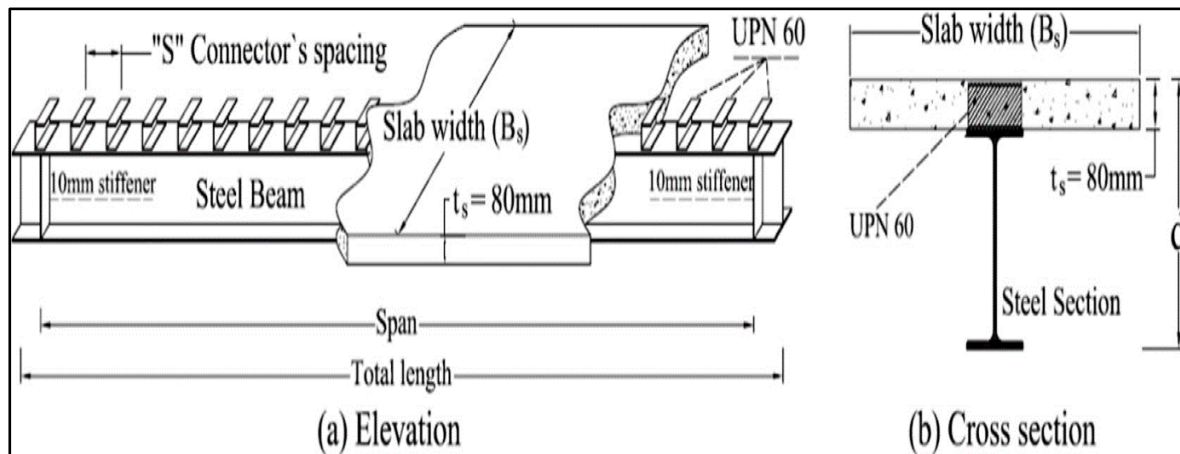
Fig. 19 Dimensions of test specimens.

Lukačević's group developed cold-formed composite steel-concrete floor systems. The suggested structural approach, LWT-FLOOR, steel built-up beams of cold-formed and connected with in-situ concrete slabs through a novel type of shear connection. In the first two phases, experimental research of lightweight floor (LWT-FLOOR) system materials and spot welds between different cold-formed sheet thicknesses is performed. Fig. 20 illustrates two possible solutions for shear connections. Full-scale LWT-FLOOR systems were tested in phases four and five of the experimental work. The tested elements' span was about 6 m, comparable to the standard spacing in floor systems of multistory buildings. As a preliminary step in the experimental work, girders without and with web openings were tested to determine the performance of built-up girders with a corrugated web made by cold-formin in the absence of concrete slabs, as illustrated in Figs. 21 and 22. Numerical models were calibrated to allow parameter-based analysis to suggest solutions. The first phase combines shear connection numerical models with probabilistic analyses to identify the best solution for shear connections. The second numerical study phase modeled built-up beams with the corrugated web with and without openings. Models calibrated for numerical calculations provide the basis for variable investigations to arrive at the most suitable solution for various web opening arrangements and longer spans. The studied geometry of the cross-section is demonstrated in Fig. 23 according to the analytical model. The concrete flange thickness was 90 mm, and its effective width measured 1000 mm. The steel grade S350 was used to construct the steel parts, and the beam's span was 6 m. The plastic neutral axis lies in a concrete flange for the proposed geometry and a complete shear connection.

The parametric finite element analysis findings demonstrated that the bending strength of the LWT-FLOOR beam specimens fabricated of cold-formed steel and the slab of concrete cast in situ was influenced by the cold-formed steel sections' resistance and the shear connection degree. In the instance of fixed end-state beam solution, the LWT-FLOOR beam's specimen resistance was limited through the steel beam's resistance, namely the spot welding. In the scenarios of pinned-state beam solution, the findings revealed that the LWT-FLOOR beam's specimen resistance was limited based on the shear connection degree. Meanwhile, increasing the spot welding (SW) counts from 2 to 3 in the region between the corrugated web and the channel flanges has no impact on the resistance of the beam. Therefore, it implies that the strength of the beam in the pinned solution was largely influenced by the stability of the cold-formed steel sections compared to the spot welds count, which had a substantial effect on the shear connection in terms of type and degree. According to previous investigations on built-up steel beam specimens containing corrugated web, it was observed that the strength was affected by the corrugated web and steel plate thickness (Lukačević, Ćurković, Rajić, & Bartolac, 2022).
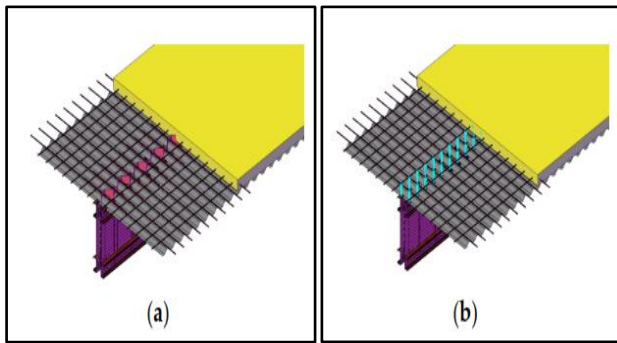
FIGURE 20: Proposed solutions for shear connection: (a) composite dowel rib connectors; (b) demountable-headed shear stud connectors
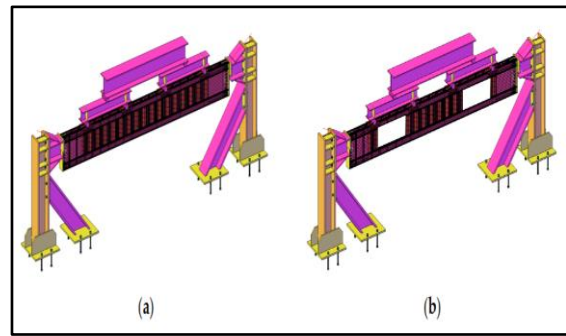
**FIGURE 21: Built-up corrugated web girder: (a) without web openings; (b) with web openings**
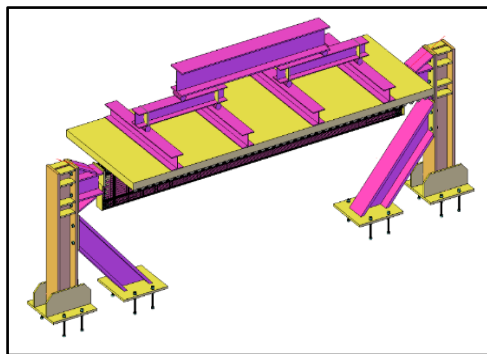
**FIGURE 22: Proposal for test set-up for LWT-FLOOR system**
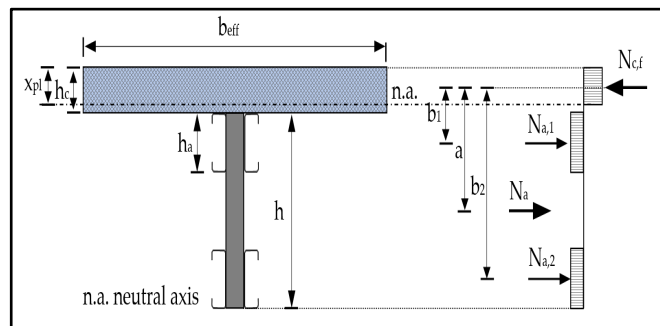
FIGURE 23: Cross-section of the analyzed LWT-FLOOR beam.

6. Numerical Analysis of Flexural Behaviour of Steel-Concrete Composite Beams

Zona and Ranzi (2011) compared three different beam models and relevant finite elements to nonlinearly analyse composite elements that interact partially. These models were developed through coupling using a shear connection with deformable properties to two Euler-Bernoulli beams (only flexural deformability and mode of failure for all components of the beam), a Euler-Bernoulli beam to a Timoshenko beam (Shear deformability was added and shear mode of failure to only one component), and two Timoshenko beams (Shear deformability was added and both components' shear modes of failure). Based on experimental data available in the literature, steel-concrete composite beams in simple supports and continuous states were employed as a reference example, as in the current study. The considerations of structural behaviour involved the shear deformability effects for a slab and steel components under different levels of load, variations in calculated collapse loads, variations of the internal actions such as forces in an axial direction, moments associated with bending, shears in the vertical direction and at the interface plane at various levels of loading. A prismatic steel-concrete composite beam is made of a reinforced concrete slab and a steel beam, as shown in Fig. 24.

The nonlinear analysis outcomes for the composite beams that fail in bending showed that the three models of beams offer an excellent approximation of those obtained from experimental tests. Therefore, models such as these are equally accurate in capturing the actual behaviour of structures. The influence of the deformability caused by shear in the steel beam was small yet not marginal in assessing the total stiffness of the structure. When the deformability in the shear of the steel beam was considered, the influence of the steel beam's shear deformability was very low and practically ignored in the estimation of the stiffness of the structure as a whole. When calculating failure load, there was no more than a 2% difference between models, or it could be neglected practically. In light of the outcomes of the nonlinear composite beams analysis experience to shear failure, it is

found that one of the models substantially exceeds in estimation of the ultimate strength of the experimental results. The variations in beams where bending and shear have interacted were substantial; consequently, ignoring the shear action in a model relating to the composite beam caused highly unreliable estimations of the structural performance. In terms of computed internal actions based on the three models of the beam, less convergence was seen for values calculated from equilibrium rather than from cross-section stresses direct integration.
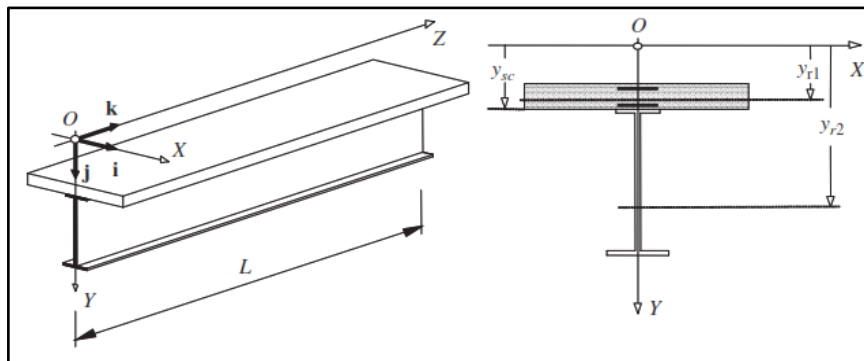
Fig. 24 Composite beam with typical shape and geometry.

Tahmasebinia, Ranzi, and Zona (2012) proposed a three-dimensional finite element model for three cases to simulate composite members using solid elements within Abaqus. Their method adopts 8-node linear brick elements (C3D8R) with reduced integration and hourglass control, avoiding the need for push-out test-based shear connector constitutive laws. Components, excluding stud heads, are meshed using structured techniques, while contact interactions between concrete, steel joists, and steel decks are modeled with surface-to-surface interaction. HARD contact and PENALTY approaches define normal and tangential responses, respectively. The embedment technique models stud-concrete and rebar-concrete interactions, where embedded nodes interpolate values from host nodes. Shear studs are tied to the steel flange using a node-to-surface TIE constraint. Steel materials follow a linear-elastic to perfectly plastic model, while concrete uses the Extended Drucker-Prager model for compression and a linear-softening approach for tension. Nonlinear behavior is captured using the RIKS method with arc-length control for complex deformation paths. In case 1, based on Chapman & Balakrishnan (1964), tests modeled included variations in mesh refinement for slabs, shear connectors, and steel components for specimen, as is given in Fig. 25. Two connector mesh types (Stud-M1 coarse and Stud-M2 fine) were considered, showing the minimal influence on results. In case 2, based on Nie, Fan, and Cai (2008), composite beams were modeled with trapezoidal profiled sheeting under various static configurations, including simply supported and continuous beams. Three slab and joist mesh levels (SB1-M1 coarse, SB1-M2 medium, SB1-M3 fine) and connector meshes (Stud-M1 and M2) were analyzed, yielding comparable outcomes, as exhibited in Fig. 26. In case 3, based on the study of Ranzi, Bradford, Ansourian, Filonov, Rasmussen, Hogan, and Uy (2009), two full-scale, simply-supported composite beams on trapezoidal steel decks with varying stud configurations (CB1: one stud per trough, CB2: two studs per trough). Beam layouts and load arrangements demonstrated the robustness of the modeling technique. The beam layout and loading arrangement are illustrated in Fig. 27.

The results for case 1 pointed out that using various refinements for a mesh of the connectors barely impacted with 1-2% when comparing the maximum calculated loads. As per case 2, using meshes Stud-M1 and Stud-M2 produces variations of about 2% in the computed forces at different deflection levels. For entire static arrangements, a good agreement was noted for the findings from numerical analyses and experimental data, referencing the proposed finite element model's capability to estimate the composite behaviour reasonably, where the maximum capacities remained at approximately 4% of the obtained data. The results of case 3 revealed that the suggested finite element model gives adequate depictions of the experimental performance. The relatively small variations in the performance of CB1 are related to the specific asymmetric load pattern implemented in the component in the first stage of testing, which had been then developed to a symmetric load configuration in the second stage, that is, deflections greater than 130 mm in the midspan. It is important to point out that the experiments ended up being stopped because of extreme deformations of the specimens and not because

specimens actually failed. As is the case here, the variations between the ultimate values obtained through the tests and those determined numerically stay at around 4%.
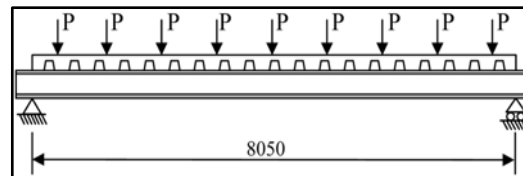

**Fig. 25 Layout of the A5 and A6 beams reported by Chapman and Balakrishnan (1964)**
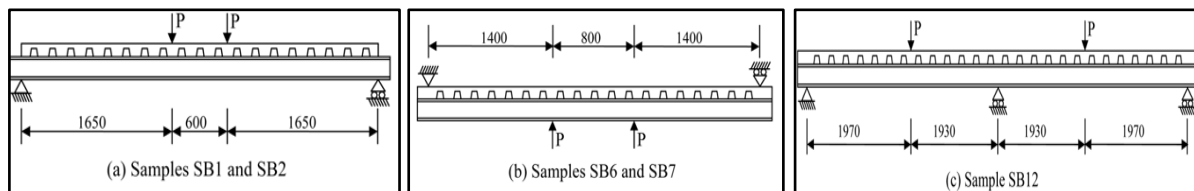
**Fig. 26 Tested beams layout reported by Nie et al. (2008)**
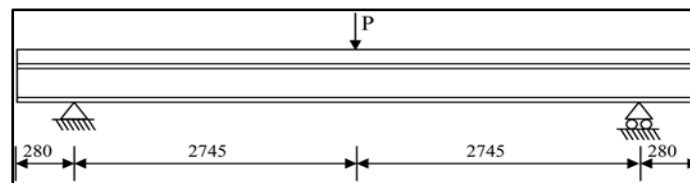
Fig. 27 Layout of beam tests reported by Ranzi et al. (2009)

Ding, Liu, Liu, Guo, and Jiang (2016) investigated the flexural stiffness of I-steel-concrete composite beam specimens in a simply supported state after being exposed to a bending moment in a positive condition by combining three approaches: experimental, standard analytical, and finite element. For the experimental approach, 14 composite beam specimens were tested, and variables involving the degree of shear connection, reinforcement percentages in transverse and longitudinal directions, and type of loading were evaluated. Fig. 28 shows a cross-section of the girder. The compressive strength fcu of concrete lay between (32-50 MPa), and coupon tests on steel plates were between (250-338 MPa) for fy and (323-350 MPa) for fu. The first type of loading was static mode and comprised two specimens. The impacts of some important parameters, namely the degree of shear connection, stud configuration and diameter, length of the beam, and method of loading, on the flexural stiffness have been investigated. The second type of applied load was dynamic cyclic mode and involved 12 remaining specimens to be tested. Additionally, three commonly employed standard codes, such as AISC, GB, and British standards, were utilized to evaluate the composite beams' flexural stiffness. Load-to-deflection curves under static loading can be employed to calculate flexural stiffness. Contrary to this, when the load is dynamic cyclic, the flexural stiffness has been obtained from secant stiffness calculations based on the enveloping curve corresponding to 40% of the peak load. The relationship between flexural stiffness and flexural rigidity of steel-concrete composite beams is defined as follows: (EI)=θ (EsItr), Where (EI) represents the calculated flexural stiffness of composite beam specimens made of steel and concrete, θ represents the coefficient of flexural stiffness, and (EsItr) refers to transformed section flexural stiffness. It represents the inertia moment for the uncracked composite transformed section. ABAQUS has been used to create models based on finite elements to simulate the performance of composite beams under flexure.

According to the outcomes of the current investigation, the experimental data demonstrated that could be modeling the studs through spring and beam elements, and both of these elements gave a good match relative to

test outcomes. Despite this, the method of spring elements demonstrates greater precision and higher computational speed than the method of a beam element. In parametric analysis using a spring element, the degree of shear connection was the primary factor affecting the coefficient of flexural stiffness. Composite beams featuring a higher shear connection possess a greater coefficient of flexural rigidity. Nevertheless, when the shear connection degree goes to 1, there is no significant increase in the coefficient of flexural stiffness. The remaining factors, like the layout of the studs in double rows, the diameter of the stud, the span of the beam, loading position, and manner, had minimal effect on the flexural stiffness. In cases where the degree of shear connection exceeded 0.5, GB 50017-2003 (National Standard of The People's Republic of China, 2003) matched FEA calculations regarding flexural stiffness. Based on AISC-LRFD (American National Standard, 2016) and BS5950-3.1(British Standard, 1990), flexural stiffness was generally greater than that calculated from FEA. The findings clarified that GB 50017-2003 provides a better prediction than the remaining standards.


| (a) For specimens SCB1-2. | (b) For specimens SCB3-14. |
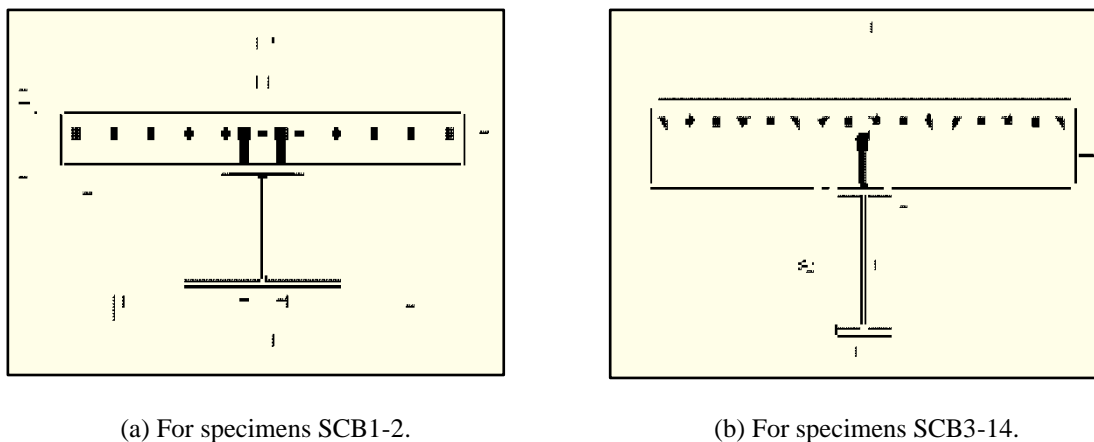
Fig. 28 Cross-section of the girder

Uddin, Alzara, Mohammad, and Yosri (2020) used higher-order beam theory (HBT) to create one-dimensional finite element models that predict the reliable response of steel–concrete composite beams. The higher-order beam model achieved this by taking a third-order variation of the longitudinal displacement over the beam depth for the steel and concrete layers separately. The shear studs made of steel employed to connect the concrete slab to the steel girder were idealized by springs distributed on an interfacial had a finite stiffness, allowing the inclusion of a composite beam partial shear interaction. The HBT offers a true parabolic response of the shear stress across the depth of the beam and, as a result, does not need a shear correction factor that may be arbitrary to estimate the total response, for example, deflection. In addition, the model could realistically predict local behaviour, such as stress distribution. For implementing HBT, models of continuous beams based on finite elements were developed according to a displacement method. The formulation of the finite element approach was created with a range compatible with complete numerical integration of the stiffness matrix to prevent a shear-lock and an oscillation problem in stress and enhance the accuracy of the solution. Four types of elements for a composite beam, namely 2-node straight, 3-node straight, 3-node isoparametric, and 3-node variably mixed, were included to establish models to identify the best number of elements of beam necessary for the best convergence. The study problem pertains to a simply supported composite beam with a T-shaped section and a length of 20,000 mm, made up of a steel I-girder and concrete slab using steel shear studs for connection, exposed to a 35 N/mm uniform load was investigated from the work of Ranzi, Gara, Leoni, and Bradford (2006) as illustrated in Fig. 29. The material characteristics of the steel girder and concrete slab were: Ec = 34.2 GPa, Gc = 14.25 GPa, Es = 210 GPa, and Gs = 84 GPa.

In this case, the problem was analyzed by HBT according to Chakrabarti, Sheikh, Griffith, and Oehlers (2013), and the collected findings were compared to those of Timoshenko's beam theory TBT and Euler-Bernoulli's beam theory EBT. In this study, the problem was used through the suggested four models based on finite element analysis, which considered the non-dimensional stiffness factor (αL) introduced by Girhammar and Pan (1993), ranging between (0.1 to 50). The deflection at the mid-extent of the span, the shear slips of the interface at the end (left side), and bending stress in the lower fiber of the section at the midpoint of the span have been estimated

using the suggested models according to HBT based on six distinct values of αL exposed to a uniform load distribution. In this study, this beam was utilized to find the behaviour of the beam when subjected to a 100 kN load at the middle point of the length to span (x = L/2) and zero length for both ends (x = 0, x = L) was investigated to evaluate the behaviour and determine the ultimate stress, slip, and deflection. The published results were used to validate the suggested models, and a two-dimensional finite element model details the composite beams' behaviour. Excellent behaviour of the proposed FE models was observed during the validation and verification in numerical analyses. Lastly, it was discovered that about thirty elements were needed for satisfactory convergence for all cases of 3-node, while the instances of 2-node called for more than fifty beam elements.
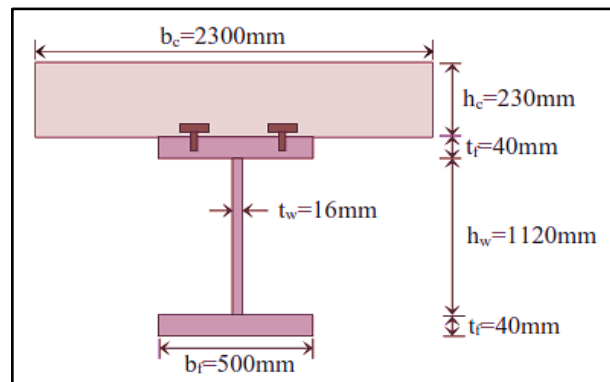

Fig. 29 Cross-section of a steel-concrete composite beam

Lacki, Derlatka, Kasza, and Gao (2021) presented the parametric investigation of a composite beam composed of steel and concrete connected by dowels. The composite beam has been modeled considering the variables determined through numerical calculations, such as the steel element mass, the vertical beam displacement, steel and concrete stresses, and the crack character of the concrete. Subsequently, in the present study, the best parametric of the beam, including dowels, was evaluated against the usually employed solution of a composite beam from steel and concrete with a shear connector and a headed stud shape. According to the numerical model, the finite element approach has been employed to explain the effect of mechanical loads on the floor beam regarding the stresses and strains. FEM-based ADINA software was utilized to perform numerical calculations. In creating the numerical model, 3D-solid elements were employed, while truss elements were adopted to model the reinforcing rebars. The slab, made of C30/37 concrete and a thickness of 160 mm, has been designed to be supported freely according to Eurocode 2 (European Committee for Standardization, 2004). Figs. 30 and 31 exhibit the dimensions of the designed composite beams and cross-section. Seven parameters have been considered for composite beams, which differ in the cross-section of steel, the cross-section of welding, the spacing between connectors, the upper and lower surfaces of the trapezoidal sheet, and the height of the connector. The control beam was designed to comply with the requirements of Eurocode 4: Composite Steel and Concrete Structures Part 1-1: General Building Rules and Regulations (European Committee for Standardization, 2004). The designed beam geometry and shear connector in stud shape have been performed, as illustrated in Fig. 32.

The numerical and analytical outcomes were not greater than the permissible values of a slab with a compressive stress-XX of 30 MPa and 235 MPa in the steel beam tensile stress-XX or 22.8mm ultimate deflection. Modifying the steel cross-section in composite beams with steel and concrete using dowel connectors does not change stress-XX degrees; however, the stress-XX levels were affected at a 90 mm height. In the case of h = 90 mm, the peak stress-XX values happened close to the midpoint of the beam span length. In the case of h = 70 mm, the maximum stress-XX levels occur near the penultimate composite dowel. Generally, stress-XX and deflection were higher for smaller cross-sections. The differences between analytical and numerical outcomes were identical in dowel beams and beams with headed studs: the difference is about 30% for compressive stress-XX in the slab, around 18% for tensile stress-XX in the steel beam, and less than 10% for maximum deflection. Regarding beams made with headed studs and dowel connectors, the steel part with dowels was 12% lighter than those containing studs.
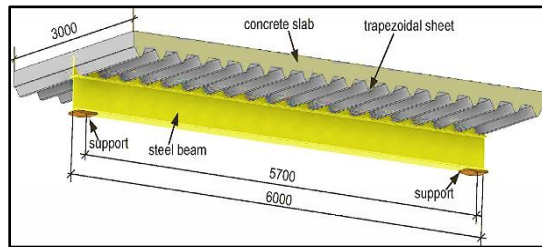
Fig. 30 Composite beam dimensions
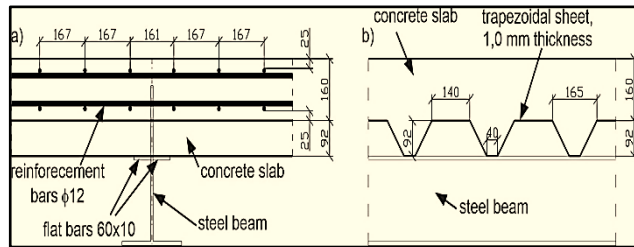
Fig. 31 Concrete slab details: a) specified spacing for reinforcement in cross-section, b) view from the side to the trapezoidal sheet T92, mm
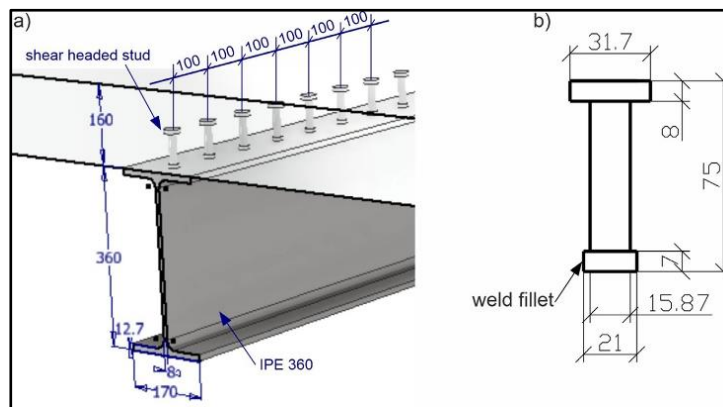

Fig. 32 Composite steel-concrete floor using shear stud connectors: (a) cross-section of beam, (b) headed stud, mm

Zheng, Li, Huang, and Wang (2021) studied the performance of steel-concrete composite beam specimens incorporating various degrees of shear connection by utilizing the program ABAQUS for finite elements. Four models of composite beams with simple supports were designed according to the experiment program using varying headed stud numbers. The specimens measured 3 m in length and featured an identical cross-section, as clarified in Fig. 34. Every steel beam with an I shape has been welded to a plate with 10 mm in thickness, a high web of 150 mm, a wide upper flange of 120 mm, and a lower flange of 160 mm wide. The concrete slabs were 80 mm high and 300 mm wide. Steel bars were numerically modeled using a T3D2 element. In contrast, the rest of the components, such as the concrete slab, the steel beam, and the headed studs, were modeled using a C3D8R element. Models based on half-beams were created to compensate against the models based on whole beams due to the symmetry of all four models. Studs and nearby concrete mesh have been optimized and densified to accurately simulate the concentration of stress from studs and nearby concrete. Fig. 35 illustrates the meshing of the FE model. "Limited sliding" has been chosen because the contact surface slip has been accounted for. Thus, the status of the contacts between nodes of the subordinate surface and the main surface was obtained through analysis. "Hard contact," as a typical option, represents the most prevalent type of normal contact. When surfaces stay in contact, they can transfer unlimited pressure. Two faces would be considered separate when the contact pressure reaches zero or negative. Regarding tangential work, Coulomb's law has been employed to determine the threshold shear stress for the models. Surfaces in contact remain bonded until the tangential stress is equal to or exceeds the threshold shear stress. "Elastic slip deformation" has been implemented in ABAQUS, and the penalty approach has been adopted to compute stiffness. For the models, the coefficient of friction has been set at 0.35 for the tangential-penalty friction between the concrete slab's bottom surface and the steel beam's top surface. A vertical displacement in a downward direction was implemented in the center of the span at a virtual reference point. The slab's top surface was coupled with the reference point to guarantee motion transfer.

The outcomes calculated using numerical simulation match well with those from the experiment data. Furthermore, the degree of shear connection significantly influences the static behavior of composite steel-concrete beams concerning load-to-deflection curve and load-to-slip development. For the static load state, the degree of shear connection of the composite steel-concrete beam considerably impacts the slip at the interface. The failure mechanisms primarily involved bending of the composite structure in the steel section failure and shear failure of the studs, which were related to the degree of connection regarding the high and low levels of connection. Additionally, the degree of connection can substantially influence the distribution of load and strain. The compression strength of concrete affected the maximum bearing strength to a specific degree; however, this effect declined as strength increased. A higher teel section of a composite beam effectively enhanced the maximum carrying capacity; however, it had little impact on the slippage at the interface relative to the maximum bearing strength. Altering the plate thickness of the steel section on the composite beam was an uneconomical approach to improving the bearing capacity compared to changing the height of the steel section of the composite beam.
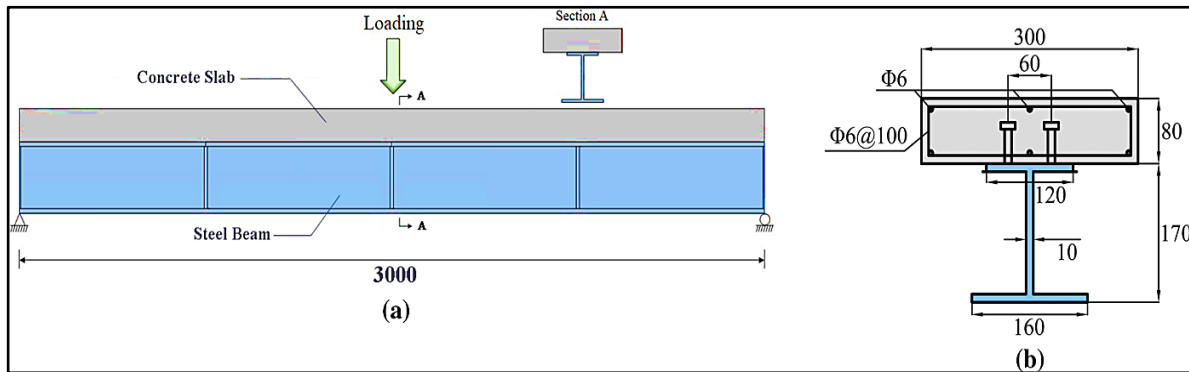

Fig. 33 Layout of finite element model: (a) in general (b) in cross-section
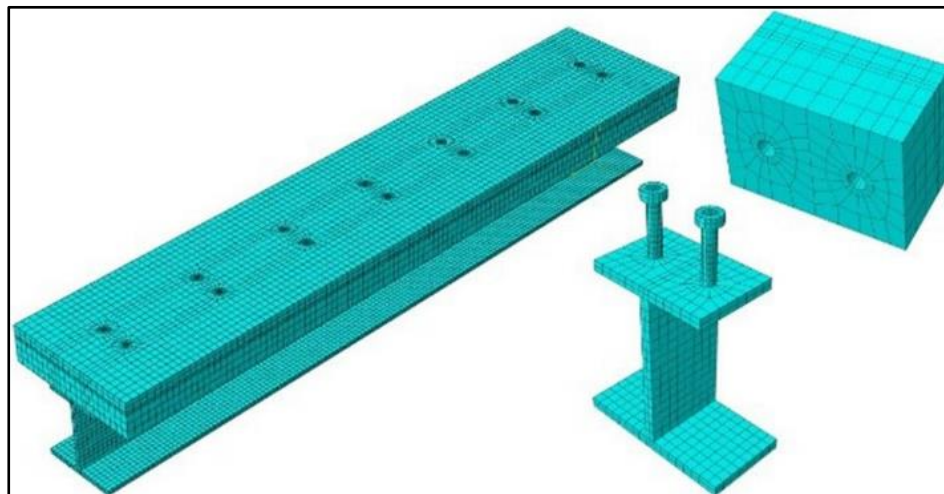

Fig. 34 The meshing in the finite element model as a complete, and for each part

7. Insights into the Performance and Characteristics of Shear Connectors, Concrete Materials, and Design Standards

Tabs. (1-3) comprehensively describe steel-concrete composite structure shear connector types, concrete materials, and codes/standards. Various connector types are summarized in terms of their performance, advantages, challenges, concrete strengths, and design standards. In addition to highlighting key features of stiffness, durability, cost-effectiveness, and applicability for modern construction practices, the classifications are based on findings from the reviewed studies.

Table 1 – Performance and characteristics of shear connectors.

Shear Connector Type	Performance	Advantages	Challenges
Headed Studs	Moderate stiffness	widely used, Ease of installation and standardization.	Limited ductility under extreme loads.
Indented Shear Connectors	High stiffness	Reduces slip and control and improves load transfer.	Complex to fabricate, higher costs.
Crestbond	High stiffness	Excellent load transfer, Expensive, reliable interaction.	Ideal for research-grade beams, Requires precise alignment during installation.
Cold-Formed U Section	Moderate capacity, less stiff,	cost-effective, Simple design, Suitable for low-cost projects.	Lower stiffness compared to hot-rolled sections.
Composite Dowels	High stiffness	Reduces weight, Innovative design, and sustainability.	The novelty of the concept limits its practical application.

Table 2 – Performance and characteristics of concrete type.

Concrete Type	Properties	Advantages	Challenges
Normal-Strength Concrete,	Moderate stiffness and strength, Economical	Widely available, Prone to cracking.	Limited ductility
High-Strength Concrete,	Higher strength	Improved cracking resistance and enhanced load-bearing capacity.	Higher cost and complexity.
Ultra-high-performance concrete (UHPC)	Exceptional stiffness and durability,	Superior durability and reduced weight	Requires skilled application, Expensive.
Steel Fiber Reinforced Concrete (SFRC),	Increased ductility	Reduced cracking, Enhanced flexural behavior, and energy dissipation	Specialized production, Higher costs.
Lightweight Concrete (LWC)	Reduced weight and Moderate stiffness	Eases structural weight limitations.	Lower stiffness than normal-weight concrete.

Table 3 – Performance and characteristics of code/standard.

Code/Standard	Focus	Strengths	Limitations
Eurocode 4	Comprehensive design for composite structures	Well-documented guidelines and validated with research.	Limited consideration of novel materials like UHPC.
AISC-LRFD	Load and resistance factor design methodology	Reliable predictions and widely used in the USA.	Limited scope for innovative designs.
GB 50017-2003	National standards for China.	Tailored to local practices and aligned with regional needs	Lacks flexibility for advanced or hybrid materials.

AS/NZS 2327	Composite construction for bridges and buildings.	Covers a wide range of scenarios and focuses on composite action.	Requires updates for new materials.
BS 5950-3.1	Traditional standards for steel structures.	-Well-suited for conventional applications and easy to implement.	Outdated in addressing modern composite design needs.

8. Conclusion

8.1. Shear Connection Design

- Fully bonded shear connectors, such as CFRP sheets or welded plates, enhance flexural capacity and stiffness compared to configurations with partial bonding or pre-debonding, which can lead to reduced performance due to crack propagation.
- Indented and hot-rolled U-section shear connectors are more effective than cold-formed or standard connectors in reducing slip and improving the interaction between steel and concrete.
- Uniform distribution of shear connectors optimizes load capacity and stiffness, while grouped or widely spaced connectors increase ductility at the expense of stiffness and strength.

8.2. Material Properties and Innovation

- Lightweight concrete reduces slab weight with negligible effects on stiffness and capacity while allowing for fewer shear connectors, which can improve ductility without compromising structural performance.
- Advanced materials like ECC, SFRC, and UHPFRC improve stiffness, flexural strength, and ductility compared to conventional concrete, and laminated UHPC layers provide additional benefits like reduced weight and cost efficiency.

8.3. Structural Performance Under Load

- A higher degree of shear connection enhances stiffness and load capacity, although improvements plateau beyond full connection.
- Partial connections are acceptable in specific design contexts.
- Failure modes vary with connection type and material configuration, transitioning from bending failure in fully interactive systems to shear connector failure in systems with lower degrees of interaction.

8.4. Numerical and Experimental Correlation

- Advanced finite element modeling techniques accurately predict structural responses and are valuable tools for optimizing shear connection designs and material configurations.
- Numerical models closely align with experimental results, validating their use in parametric studies and predicting global and local structural behavior.

8.5. Innovative Configurations

- Prefabricated beams with segmented precast slabs exhibit reduced stiffness and ductility compared to monolithic slabs, though design adjustments, such as modifying gap widths or slab dimensions, can mitigate these effects.
- Cold-formed steel beams with optimized shear connections demonstrate suitability for long spans, with performance influenced by connection stability and component geometry.

Code and Design Implications:

- Current design codes such as Eurocode-4, AISC, and GB 50017-2003 provide reliable predictions for composite beam behavior. However, adjustments may be needed to accommodate strain-hardening effects in stainless steel and better address shear connection design nuances.

9. Common Points and Focuses of Studies

The reviewed studies collectively emphasize the critical factors influencing the performance of steel-concrete composite beams, with a significant focus on shear connection design, material properties, and structural behavior. Shear connectors, particularly indented, hot-rolled U-sections and grouped connectors, are pivotal in ensuring efficient load transfer and minimizing slip, with spacing and distribution playing key roles in balancing stiffness and ductility. Material innovations, including lightweight concrete, engineered cementitious composites (ECC), steel fiber-reinforced concrete (SFRC), and ultra-high-performance concrete (UHPC), improve stiffness, strength, and ductility while reducing self-weight and promoting sustainability. Failure modes vary based on connection degree and material type, typically transitioning from bending failure in fully connected systems to shear connector deformation in partially connected configurations. Numerical modeling, validated against experimental results, consistently accurately predicts load-deflection behavior, slip, and stress distribution, serving as a vital tool for optimizing beam design and configuration. Though innovative, prefabricated and segmented slab systems exhibit reduced stiffness and ductility compared to monolithic designs, requiring adjustments such as modifying slab gaps or girder dimensions to maintain performance. Higher degrees of shear connection generally enhance stiffness and load capacity but gain plateau beyond full connection. Load-deflection and slip behavior are closely linked to connector spacing, with shorter spacing ensuring monolithic performance. Design codes like Eurocode-4 and AISC generally align with experimental findings, though modifications may be necessary for unique materials like stainless steel and non-standard connection designs.

10. General Gaps in the Studies

- **Static vs. Dynamic Loading**: Most research focuses on static loading, with limited exploration of dynamic, cyclic, or impact loads. This leads to uncertainties about performance under real-world conditions such as earthquakes or traffic-induced vibrations.
- **Long-Term Effects**: Creep, shrinkage, and fatigue are insufficiently studied, particularly for innovative materials like ECC, SFRC, and UHPC, which require validation under combined environmental and mechanical stresses.
- **Prefabricated and Segmented Systems**: Prefabricated and segmented slab systems show reduced stiffness and ductility compared to monolithic systems, and strategies to address these deficiencies remain underexplored.
- **Shear Connector Diversity:** Research predominantly focuses on specific shear connectors (e.g., indented or bolted), with alternative or hybrid designs and performance under harsh conditions (e.g., high temperatures, corrosive environments).
- **Design Code Validation:** Findings are often validated against specific design codes (e.g., Eurocode-4, AISC), with limited consideration of regional variations and broader applicability.
- **Sustainability Assessments:** Sustainability evaluations are confined to material-level improvements and lack comprehensive life-cycle analyses to balance environmental impact, performance, and cost.
- **Multi-Axial Loading:** Few studies investigate multi-axial loading scenarios, such as combined bending, shear, and torsion, essential for understanding performance in complex structural systems.

11. Inconsistencies and Conflicting Findings

The literature on steel-concrete composite beams reveals several inconsistencies and variations in findings. The following is a synthesis of conflicting results and their possible causes:

- **Shear Connector Performance:** Sallam et al. (2010) highlighted reduced flexural capacity with partial bonding or pre-debonding configurations. In contrast, Zhou et al. (2021) found that bolted connectors provided comparable ultimate resistance to welded studs despite reduced stiffness.

Reason: Bolted connectors provide mechanical redundancy over adhesive bonding, which is more prone to debonding. When debonding starts, adhesive connections fail abruptly, while bolted connections fail gradually. Four-point bending likely amplified the effects of partial bonding, whereas broader loading scenarios distributed stresses more evenly.

- **Material Influence on Structural Behavior:** Studies by Muteb and Rasoul (2016) and Liu et al. (2020) reported that advanced materials like UHPC significantly enhance load capacity and stiffness. However, Hamoda et al. (2017) observed mixed results for engineered cementitious composites (ECC) and fiber-reinforced concrete (SFRC), with ECC showing superior ductility but lower stiffness than SFRC.

Reason: Due to its dense matrix, ECC emphasizes ductility and strain-hardening at the expense of stiffness. The microfiber properties of SFRC result in a higher stiffness but a lower ductility; in hybrid systems like those, varying stiffness materials interact, resulting in a mixed performance. When the material is loaded under negative moments or other conditions, its strengths or weaknesses may be amplified.

- **Failure Modes and Degree of Interaction**: Several studies (e.g., Yang et al. (2023) and Zhou et al., (2021)) indicate that higher shear connection degrees enhance stiffness and capacity. However, Valente (2007) showed that partial connections, while reducing stiffness, can increase ductility, making them suitable for specific applications.

Reason: A high shear connection degree maximizes stiffness and load capacity by enforcing composite action but sacrifices ductility. Partial connections enhance ductility at the expense of stiffness and capacity. Depending on the intended application and loading conditions, both approaches have advantages.

- **Numerical vs. Experimental Validations**: Alves et al. (2018) achieved high alignment between numerical and experimental results in predicting beam behavior, while others (e.g., Zheng et al. (2021)) noted discrepancies at higher loads or slip conditions due to limitations in numerical assumptions.

Reason: Zheng et al., 2021 dealt with more complex and variable conditions than Alves et al. (2018). While Alves et al. (2018) studied elastic-plastic behavior, Zheng et al., 2021 studied performance up to failure, where nonlinearities dominate. In Alves et al. (2018), indented connectors minimized slip, simplifying predictions, whereas Zheng et al., 2021 showed significant slip, complicating modeling.

- **Prefabricated vs. Monolithic Systems:** Prefabricated beams studied by Yang et al. (2023) demonstrated reduced stiffness and ductility compared to monolithic designs. Conversely, prefabricated systems are often advocated for their speed and sustainability.

Reason: Based on Yang et al.'s (2023) study, prefabricated beams show reduced stiffness and ductility compared to monolithic designs because of segmented interfaces and complex connections that cause slip and localized stress accumulation. Consequently, these factors weaken the composite action and reduce the system's ability to transfer loads uniformly. Although prefabricated systems are highly valued for their speed and sustainability, they reduce on-site labor, reduce material waste, and enable precise quality control under factory conditions (Lukačević et al., 2016).

12. Recommendations for Further Studies

- Investigate long-term performance under sustained and cyclic loads, including fatigue, creep, and shrinkage effects.
- Develop advanced shear connector designs and materials for improved bond strength and corrosion resistance.
- Explore the effects of environmental factors and hybrid concretes (e.g., UHPC, ECC, and lightweight concrete) on structural performance.

- Enhance numerical modeling techniques, including dynamic effects, sensitivity analyses, and AI-based optimization.
- Integrate sustainable materials (e.g., recycled aggregates, green concrete) to reduce environmental impact.
- Validate findings with large-scale experimental studies and optimize cost-benefit ratios for composite configurations.
- Investigate innovative construction methods like additive manufacturing and prefabrication for efficiency and speed.

References

Alves, A. R., Isabel, B. V., Washintgon, B. V., & Gustavo, S. V. (2018). Prospective study on the behaviour of composite beams with an indented shear connector. *Journal of Constructional Steel Research*, *148*, 508-524.

American National Standard. (2016). *Specification for Structural Steel Buildings* (ANSI/AISC 360-16). AMERICAN INSTITUTE OF STEEL CONSTRUCTION, Chicago, Illinois. https://www.aisc.org/

Ataei, A., Bradford, M. A., & Liu, X. (2016). Experimental study of composite beams having a precast geopolymer concrete slab and deconstructable bolted shear connectors. Engineering Structures, 114, 1-13.

Australian/New Zealand Standard. (2017). *Composite Structures‐Composite Steel‐Concrete Construction in Buildings* (AS/NZS 2327: 2017). Standards New Zealand. https://www.standards.govt.nz/

Bärtschi, R. (2005). Load bearing behaviour of composite beams in low degrees of partial shear connection (No. 290). vdf Hochschulverlag AG.

British Standard. (1990). *Structural use of steelwork in building- Part 1. Code of practice for design in simple and continuous construction: hot rolled sections* (BS 5950: Part 1: 1990). British standard Institution. https://www.bsigroup.com/en-GB/.

Chakrabarti, A., Sheikh, A. H., Griffith, M., & Oehlers, D. J. (2013). Dynamic response of composite beams with partial shear interaction using a higher-order beam theory. *Journal of Structural Engineering*, *139*(1), 47-56.

Chapman, J. C., & Balakrishnan, S. (1964). Experiments on composite beams. *The Structural Engineer*, *42*(11), 369-383.

Choi, W., Choi, Y., & Yoo, S. W. (2018). Flexural Design and Analysis of Composite Beams with Inverted-T Steel Girder with Ultrahigh Performance Concrete Slab. *Advances in Civil Engineering*, *2018*(1), 1356027.

Daou, A., Mahayri, A. R., Daou, Y., Baalbaki, O., & Khatib, M. (2021). The Use of Shear Connectors for Enhancing the Performance of Steel–Concrete Composite Beams: Experimental and Numerical Assessment. *International Journal of Steel Structures*, *21*, 1966-1976.

Ding, F. X., Liu, J., Liu, X., Guo, F. Q., & Jiang, L. Z. (2016). Flexural stiffness of steel-concrete composite beam under positive moment. *Steel and Composite Structures*, *20*(6), 1369-1389.

Döinghaus, P. (2001). *Zum Zusammenwirken hochfester Baustoffe in Verbundkonstruktionen* [Doctoral dissertation, Institute of Structural Concrete, RWTH Aachen).

Du, H., Hu, X., Meng, Y., Han, G., & Guo, K. (2020). Study on composite beams with prefabricated steel bar truss concrete slabs and demountable shear connectors. Engineering Structures, 210, 110419.

Dujmovic, D., Androic, B., & Lukacevic, I. (2015). Composite Structures According to Eurocode 4: Worked Examples. John Wiley & Sons.

European Committee for Standardization. (2004). *Eurocode 2: Design of concrete structures–Part 1-1: General rules and rules for buildings* (BS EN 1992-1-1+A1). British Standard Institution. https://knowledge.bsigroup.com/

European Committee for Standardization. (2004). *Eurocode 4: Design of Composite Steel and Concrete Structures—Part 1-1: General Rules and Rules for Buildings* (EN 1994-1-1). CEN and CENELEC. https://www.cencenelec.eu/european-standardization/european-standards/

Ferreira, F. P. V., Tsavdaridis, K. D., Martins, C. H., & De Nardin, S. (2021). Steel-concrete composite beams with precast hollow-core slabs: A sustainable solution. Sustainability, 13(8), 4230.

Girhammar, U. A., & Pan, D. (1993). Dynamic analysis of composite members with interlayer slip. *International Journal of Solids and Structures*, *30*(6), 797-823.

Hamoda, A., Hossain, K. M. A., Sennah, K., Shoukry, M., & Mahmoud, Z. (2017). Behaviour of composite high performance concrete slab on steel I-beams subjected to static hogging moment. *Engineering Structures*, *140*, 51-65.

Hegger, J., Sedlacek, G., Döinghaus, P., Trumpf, H., & Eligehausen, R. (2001). Studies on the ductility of shear connectors when using high-strength steel and high-strength concrete. In *International symposium on connections between steel and concrete* (pp. 1025-1045). RILEM Publications SARL.

Henderson, I. E. J., Zhu, X. Q., Uy, B., & Mirza, O. (2015). Dynamic behaviour of steel–concrete composite beams with different types of shear connectors. Part I: Experimental study. Engineering Structures, 103, 298-307.

Jakovljević, I., Spremić, M., & Marković, Z. (2023). Methods for life extension of multi-storey car park buildings. Structural Engineering International, 33(2), 314-324.

Johnson, R. P., & Anderson, D. (2004). *Designers' guide to EN 1994-1-1: eurocode 4: design of composite steel and concrete structures. General rules and rules for buildings*. Thomas Telford.

Lacki, P., Derlatka, A., Kasza, P., & Gao, S. (2021). Numerical study of steel–concrete composite beam with composite dowels connectors. *Computers & Structures*, *255*, 106618.

Lasheen, M., Shaat, A., & Khalil, A. (2016). Behaviour of lightweight concrete slabs acting compositely with steel I-sections. *Construction and Building Materials*, *124*, 967-981.

Lin, Z., Liu, Y., & Roeder, C. W. (2016). Behavior of stud connections between concrete slabs and steel girders under transverse bending moment. Engineering Structures, 117, 130-144.

Liu, J., Lai, Z., Chen, B., & Xu, S. (2020). Experimental behavior and analysis of steel-laminated concrete (RC and UHPC) composite girders. *Engineering Structures*, *225*, 111240.

Lukačević, I., Ćurković, I., Rajić, A., & Bartolac, M. (2022). Lightweight composite floor system—cold-formed steel and concrete—LWT-FLOOR project. *Buildings*, *12*(2), 209.

Ma, S., Lou, Y., & Bao, P. (2022). Experimental research and numerical analysis of shearing resistance in steel-concrete composite beam connectors. Case Studies in Construction Materials, 17, e01210.

Mosallam, A. S., Feo, L., Elsadek, A., Pul, S. E. L. İ. M., & Penna, R. (2014). Structural evaluation of axial and rotational flexibility and strength of web–flange junctions of open-web pultruded composites. Composites Part B: Engineering, 66, 311-327.

Muteb, H. H., & Rasoul, Z. M. A. (2016). Behavior of composite ultra high performance concrete-steel beams (experimental and finite element analysis studies). *Journal Of Kerbala University*, *14*(2).

National Standard of The People's Republic of China. (2003). *Code for Design of Steel Structures* (GB 50017-2003). The Standardization Administration of the People's Republic of China. https://www.gbstandards.org/China_standard_english.asp?code=GB%2050017-2003.

Nie, J., Fan, J., & Cai, C. S. (2008). Experimental study of partially shear-connected composite beams with profiled sheeting. *Engineering Structures*, *30*(1), 1-12.

Oehlers, D. J., & Bradford, M. A. (1995). *Composite steel and concrete structural members: Fundamental behaviour* (1st ed.). Pergamon, Oxford.

Oehlers, D. J., Nguyen, N. T., Ahmed, M., & Bradford, M. A. (1997). Partial interaction in composite steel and concrete beams with full shear connection. *Journal of Constructional Steel Research, 41*(2-3), 235-248.

Park, Y. H., Kim, S. H., Lee, S. Y., & Choi, J. H. (2013). Approximate analysis method for composite beams with partial interaction using Fourier series. *International Journal of Steel Structures,* 13, 219-227. https://doi.org/10.1007/s13296-013-2002-9.

Ranzi, G., Bradford, M. A., Ansourian, P., Filonov, A., Rasmussen, K. J. R., Hogan, T. J., & Uy, B. (2009). Full-scale tests on composite steel–concrete beams with steel trapezoidal decking. *Journal of Constructional Steel Research*, *65*(7), 1490-1506.

Ranzi, G., Gara, F., Leoni, G., & Bradford, M. A. (2006). Analysis of composite beams with partial shear interaction using available modelling techniques: A comparative study. *Computers & structures*, *84*(13-14), 930-941.

Ribeiro Neto, J. G., Vieira, G. S., & Zoccoli, R. D. O. (2020). Experimental analysis of the structural behavior of different types of shear connectors in steel-concrete composite beams. *Revista IBRACON de Estruturas e Materiais*, *13*, e13610.

Sallam, H. E. M., Badawy, A. A. M., Saba, A. M., & Mikhail, F. A. (2010). Flexural behavior of strengthened steel–concrete composite beams by various plating methods. *Journal of Constructional Steel Research*, *66*(8-9), 1081-1087.

Shao, X., Deng, L., & Cao, J. (2019). Innovative steel-UHPC composite bridge girders for long-span bridges. Frontiers of Structural and Civil Engineering, 13, 981-989.

Su, Q., Yang, G., & Bradford, M. A. (2015). Behavior of a continuous composite box girder with a prefabricated prestressed-concrete slab in its hogging-moment region. Journal of Bridge Engineering, 20(8), B4014004.

Tahmasebinia, F., Ranzi, G., & Zona, A. (2012). Beam tests of composite steel-concrete members: A three-dimensional finite element model. *International Journal of Steel Structures*, *12*, 37-45.

Uddin, M. A., Alzara, M. A., Mohammad, N., & Yosri, A. (2020, October). Convergence studies of finite element model for analysis of steel-concrete composite beam using a higher-order beam theory. In *Structures* (Vol. 27, pp. 2025-2033). Elsevier.

Valente, I. (2007). *Experimental studies on shear connection systems in steel and lightweight concrete composite bridges* [Doctoral dissertation, University of Minho]. https://hdl.handle.net/1822/8478.

Valente, I., & Cruz, P. J. (2010). Experimental analysis on steel and lightweight concrete composite beams. *Steel and Composite Structures*, 83-90. DOI:10.12989/scs.2010.10.2.169.

Vasdravellis, G., Uy, B., Tan, E. L., & Kirkland, B. (2012). The effects of axial tension on the hogging-moment regions of composite beams. *Journal of Constructional Steel Research*, *68*(1), 20-33.

Veríssimo, G. S. (2007). Development of an indented rib shear connector for steel-concrete composite structures and an investigation of its structural behaviour. *Federal University of Minas Gerais, Belo Horizonte, Brazil*.

Wald, F., Zadonini, R., & Jaspart, J. P. (2000). The European steel design educational programme for the czechoslovak praxis. In *Symposium transfer of technologies 2000*.

Wang, W., Zhang, X. D., Zhou, X. L., Zhang, B., Chen, J., & Li, C. H. (2022). Experimental study on shear performance of an advanced bolted connection in steel-concrete composite beams. Case Studies in Construction Materials, 16, e01037.

Yang, T., & Xie, R. (2023). Flexural behaviors of prefabricated composite beams with segmented precast concrete slabs. Journal of Constructional Steel Research, 201, 107692.

Yang, T., Zhou, X., & Liu, Y. (2023). Flexural performance of prefabricated composite beams with grouped bolt shear connectors under positive bending moments. *Engineering Structures*, *277*, 115387.

Yoo, S. W., & Choo, J. F. (2016). Evaluation of the flexural behavior of composite beam with inverted-T steel girder and steel fiber reinforced ultra high performance concrete slab. *Engineering Structures*, *118*, 1-15.

Yoo, S. W., Choi, Y. C., Choi, J. H., & Choo, J. F. (2021). Nonlinear flexural analysis of composite beam with Inverted-T steel girder and UHPC slab considering partial interaction. *Journal of Building Engineering*, *34*, 101887.

Zeng, X., Jiang, S. F., & Zhou, D. (2019). Effect of shear connector layout on the behavior of steel-concrete composite beams with interface slip. *Applied Sciences*, *9*(1), 207.

Zheng, X., Li, W., Huang, Q., & Wang, B. (2021). Finite element modeling of steel-concrete composite beams with different shear connection degrees. *International Journal of Steel Structures*, *21*(1), 381-391.

Zhou, Y., Uy, B., Wang, J., Li, D., Huang, Z., & Liu, X. (2021). Behaviour and design of stainless steel-concrete composite beams. *Journal of constructional steel research*, *185*, 106863.

Zona, A., & Ranzi, G. (2011). Finite element models for nonlinear analysis of steel–concrete composite beams with partial interaction in combined bending and shear. *Finite Elements in Analysis and Design*, *47*(2), 98-118.